A comprehensive review on photovoltaic emulator

Razman Ayop, Chee Wei Tan*

Department of Electrical Power Engineering, Faculty of Electrical Engineering, Universiti Teknologi Malaysia, UTM, 81310 Skudai, Johor, Malaysia

ARTICLE INFO

ABSTRACT

The photovoltaic (PV) emulator is a nonlinear power supply which has similar current-voltage (I-V) characteristic to the PV module. In solar energy generation research, such as the maximum power point tracking (MPPT) and the PV inverter, the actual PV module and the high power controllable light source were used during the experimenting phase. However, this method requires complex experiment setup, is highly inefficient, and can damage the PV module. The PV emulator provides a simpler and more efficient solution compared to the actual PV module and the controllable light source while maintaining similar output produces by the actual PV module. This paper provides a template for the researcher to design the PV emulator according to the requirements established from the tested system. The PV emulator consists of three parts which are the PV model, the control strategy, and the power converter. The PV model produces the I-V characteristic of the PV module. The control strategy determines the operating point of the PV emulator on the I-V characteristics curve and produces the reference signal for the power converter. The power converter follows the reference signal and generates a similar output as the actual PV module.

1. Introduction

A recent study shows the potential of the solar based energy generation using the Photovoltaic (PV) panel to fulfill the world's energy demand. Solar energy is one of the renewable energies that requires little maintenance, has a low operation cost, and does not pollute. Up until 2015, there was a 50 GW increase annually in the global PV energy production, which totaled up to 227 GW of estimated global capacity of the PV energy [1]. This shows a 22% increase in the global energy production from the PV generation based system. Malaysia has the potential for solar based energy generation due to its high and steady irradiance throughout the year [2]. As a result, there was a 245% increase in the PV energy production in Malaysia from 2013 to 2014 [3]. The rise in PV's popularity is due to an increase in awareness of the PV's potential, government programs to promote the use of the renewable energy, and the increase in the market competition of the PV.

One of the components in the PV energy generation system is the maximum power point tracking (MPPT). Since the PV module has nonlinear output, the MPPT ensures the maximum power is extracted from the PV module. In the development stage of the MPPT, the PV module is emitted with the irradiance from the controllable halogen lamp or the light emitting diode (LED) to test the effectiveness of the MPPT [4]. However, the setup for this test bed is complex and temperature manipulation is not flexible. This method also requires a large area for the actual PV module, the light source, and a controllable direct current (DC) or alternating current (AC) source to control the light source. Besides, this method is inefficient since a high power is required by the light source to produce irradiance for the PV module. Another available test bed option for MPPT device testing is the PV emulator.

The PV emulator is a nonlinear power supply capable of producing the current-voltage (I-V) characteristic of the PV module. The PV emulator functions as a power source in the experimental stage of the solar energy generating system to allow repeatable testing conditions. The PV emulator offers a more convenient control of ambient conditions rather than complex irradiance and temperature control to allow faster and more efficient solar energy generation system testing. The PV emulator available in the market varies from a single panel emulation (approximately 300 W) to a PV array emulation (larger than 300 W). However, this type of PV emulator is expensive, ranging from $ 6385 (Elgar ETS60X14C-PVF) to $ 21,000 (Magna Power TSD50050240) [5,6]. Therefore, much research related to the PV emulator has been conducted to reduce the overall cost and improve the dynamic response of the PV emulator.

There are several control strategies used for the PV emulator. The direct referencing method is commonly used in the PV emulator due to its simplicity [7–12]. The hybrid-mode controlled method [13–15] and the resistance comparison method [16–18] produce a stable output for the PV emulator at any load condition. The hill climbing method for the PV

---

emulator is easily designed since a compensator is not used [19,20]. The analog based method does not have computational delay and the partial shading condition is easily emulated [9,21–24]. Besides the control strategy, the implementation of the PV model is also improved for the PV emulator. The PV model increases the computational delay and results in incorrect output for the PV emulator. To reduce the calculation burden of the PV model in the PV emulator control system, the PV model is simplified [11,12,25–27], changed to the look-up table [28–33], applied with the piecewise linear method [34–37], or trained using the neural network method [12,38]. The power converter is a part of the PV emulator system. The switched-mode power supply (SMPS) is commonly used in the PV emulator and is highly efficient [17,18,33,39,40]. The linear regulator is useful if the output ripple for the PV emulator needs to be removed [13,41–43]. The design of the PV emulator using the program-mable power supply is simple since the closed-loop system for the power converter is already included in the system [15,44,45].

Much research has been conducted on the PV emulator. However, there are no specific papers that compile and discuss the techniques and control strategies for the PV emulator. The objectives of this paper are to review the PV emulator system that consists of the PV model, the control strategy, and the power converter. A review of the PV emulator is important to begin research on the PV emulator. This paper is organized as follows, where the next section describes the overview of the PV emulator which consists of three parts namely the PV model, the control strategy, and the power converter system. The next section describes two types of PV models used in the PV emulator application and the PV model implementation method inside the controller. The control strategy discusses the available method, partial shading im-plementation, and the hardware platform used for the PV emulator. The topology, the continuous current mode, the ripple factor, the small signal analysis, and the PID controller for the power converter system used in the PV emulator application are also discussed.

2. Overview of photovoltaic emulator

There are three parts in the PV emulator system introduced by the researcher, as shown in Fig. 1. The first part of the PV emulator system is the PV model. The function of the PV model is to produce the I-V characteristics of the PV module signal. This signal is used by the closed-loop power converter system to emulate the characteristic of the PV module. The PV model is highly responsible for the accuracy of the PV emulator; however, the PV emulator requires real-time calculations of the PV model to operate properly. Therefore, the PV model used in the PV emulator application must remain simple without compromis-ing the accuracy of the I-V characteristics produced.

The second part of the PV emulator system is the control strategy. The control strategy of the PV emulator is the method used to interface the PV model with the closed-loop power converter system. The control strategy is responsible for finding the operating point of the PV emulator. The control strategy combines the PV model with the closed-loop power converter system to become the PV emulator. A good control strategy should be able to accurately follow the signal produced by the PV model, create a stable PV emulator output, require low processing burden, capable of emulating various types of PV modules without the need to redesign the whole control strategy (adaptability), and does not affect the closed-loop power converter system or the load (independency).

The third part of the PV emulator system is the power converter. The power converter is used to change the I-V characteristic signal produced by the PV model into the I-V characteristic capable of transmitting power. The power converter affects the dynamic perfor-mance and the efficiency of the PV emulator. The actual PV module dynamic response is approximately a 10th of a microsecond [46]. Therefore, a good PV emulator needs to have a similar dynamic response to the actual PV module.

3. Photovoltaic model

There are two considerations in the PV model used for the PV emulator. The first consideration is the types of PV models used, of which there are two. The models are the electrical circuit model and the interpolation model, as shown in Fig. 2. The second consideration is the methods used to implement the PV model inside the controller of the PV emulator; there are five of these methods, as shown in Fig. 2, which include direct calculation method, look-up table method, piece-wise linear method, neural network method, and curve segmentation method.

3.1. Type of photovoltaic model

3.1.1. Electrical circuit model

The electrical circuit model is the PV modeling represented in the form of an electrical circuit and the PV characteristic equation is derived using the Kirchhoff current law [47]. This model is also known as the analytical model and is commonly used in the PV emulator application. The single diode model and the double diode model are two types of electrical circuit models. The single diode model shown in Fig. 3 is also known as the single diode model with a series and a shunt resistor, the 1D2R model or the five parameter model [17,26,42,48–55]. While the double diode model shown in Fig. 4 is also known as the
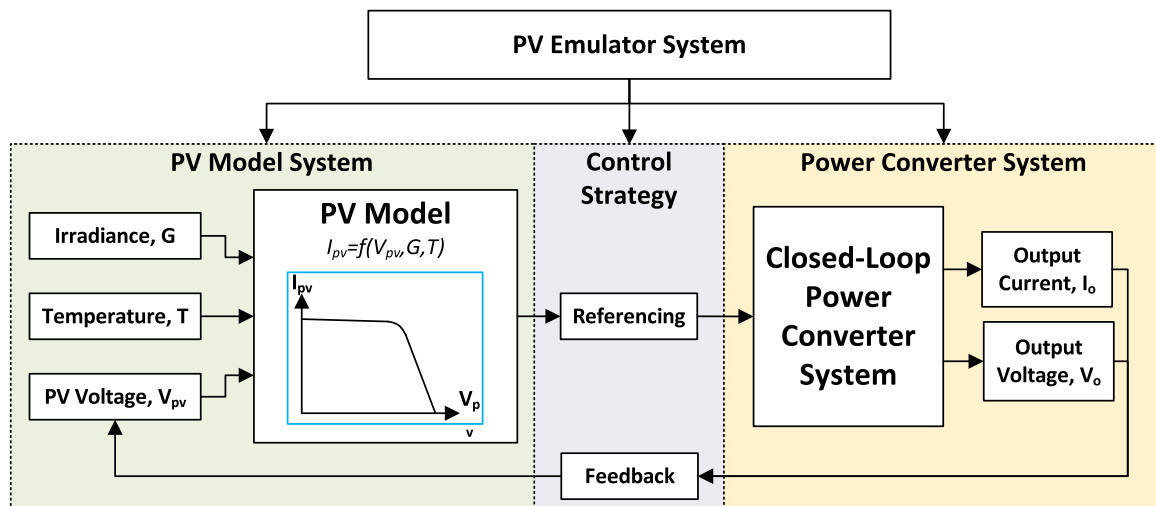

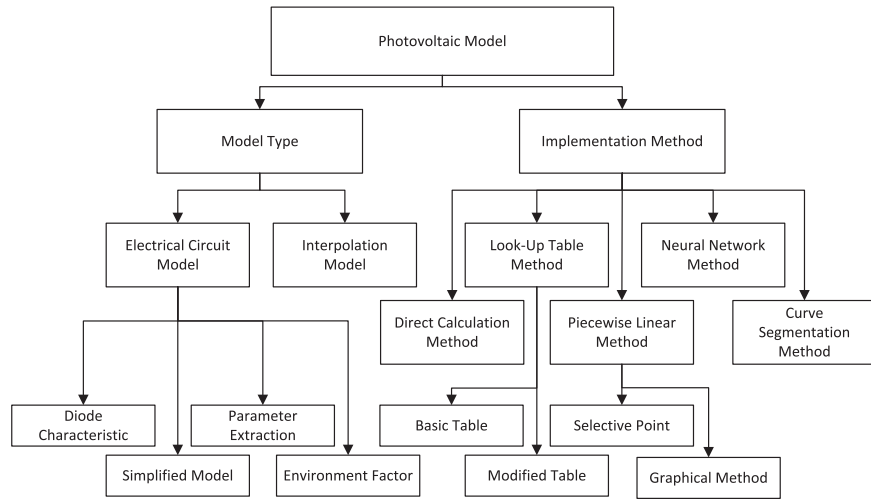Fig. 1. The three parts of the PV emulator system.

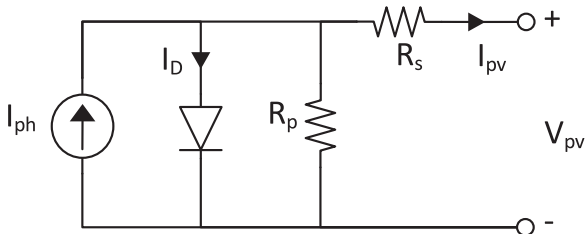Fig. 2. PV model overviews in the PV emulator application.

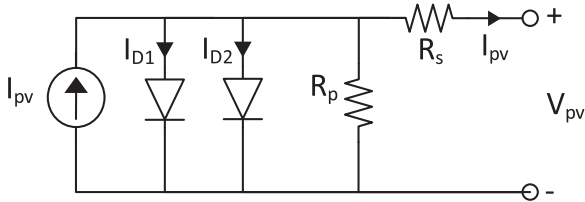Fig. 3. Circuit representation of the single diode model (1D2R Model).

Fig. 4. Circuit representation of the double diode model (2D2R Model).

double diode model with a series and a shunt resistor, the 2D2R model, or the eight parameter model [21,56–65]. The single diode model is commonly used in the PV emulator application due to its simplicity and accuracy [9,17,24,26,36,40,42,45,48–50,66–71], while the double diode model is rarely used for the PV emulator [21,58].

3.1.1.1. Diode type. The single diode model is represented as Eq. (1) and the circuit representation is shown in Fig. 3 [63].

$$I_{pv} = I_{ph} - I_s \left[e^{\frac{V_{pv} + I_{pv}R_s}{AV_T}} - 1 \right] - \frac{V_{pv} + I_{pv}R_s}{R_p} \tag{1}$$

where I_{pv} is the PV module current, I_{ph} is the photo-generated current or the photocurrent, I_s is the saturation current, A is the ideality factor (also known as the diode quality factor or the n-factor), R_s is the PV module series resistance, V_{pv} is the PV module voltage, and R_p is the PV module shunt resistor.

The double diode model is represented in Eq. (2) and the circuit representation is shown in Fig. 4.

$$I_{pv} = I_{ph} - I_{s1} \left[e^{\frac{V_{pv} + I_{pv}R_s}{AV_T}} - 1 \right] - I_{s2} \left[e^{\frac{V_{pv} + I_{pv}R_s}{2V_T}} - 1 \right] - \frac{V_{pv} + I_{pv}R_s}{R_p} \tag{2}$$

where I_{s1} is the dark saturation current due to the diffusion mechanism and I_{s2} is the dark saturation current due to recombination in the space-charge layer.

3.1.1.2. Simplified model. The single diode model is simplified by removing the parasitic resistance from the equation. This type of model is called the single diode model with a series resistance or the 1D1R model [12,18,25,39,72–81], and the circuit representation is shown in Fig. 5(a). This model excludes the parallel resistance from the equation (the value of R_p in Eq. (1) is set to infinity). There is also the ideal model or the 1D model used in the PV emulator application [31,41,69,82]. This type of model does not include the parasitic resistance, as shown in Fig. 5(b) and the characteristic equation is shown in Eq. (3). This type of model is inaccurate since the series resistance highly affects the PV module output [47,83].

$$I_{pv} = I_{ph} - I_s \left[e^{\frac{V_{pv}}{AV_T}} - 1 \right] \tag{3}$$

3.1.1.3. Parameter extraction. The parameter extraction, or also known as the parameter estimation, is used when the theoretical parameters such as I_{ph}, I_s, R_s, R_p, and A are unavailable [47,84,85]. The parameter extraction is done by using two methods, which are by using the selected value from I-V and P-V characteristic curve of PV module or is based on an algorithm that fits the I-V characteristic graph of PV cell [64,65].
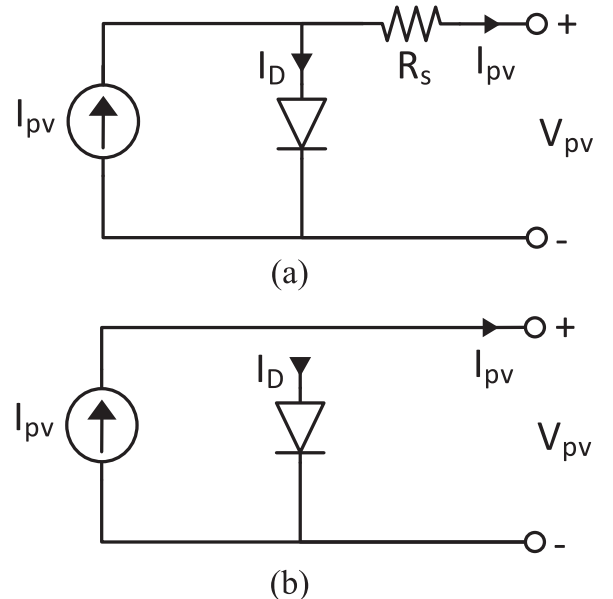

(a)

(b)

Fig. 5. The circuit representation of the simplified single diode model. a) The single diode model with a series resistor (1D1R Model). b) The ideal Model (1D Model).

The parameter extraction that uses selective points to determine the theoretical parameters requires the open circuit voltage (V_{oc}), the short circuit current (I_{sc}), the maximum power voltage (V_{mp}), and the maximum power current (I_{mp}) [51,60,71,84,86]. Examples of the methods used in the parameter extraction that use selective points are the Bacteria Foraging Algorithm [66] and the Conjugate Gradient Optimization Method [86]. Although these methods are simple, the inaccurate measurement of the selective point significantly affects the PV model accuracy [64]. The curve fitting method uses all the data from the I-V characteristic curve to extract the theoretical parameter. This method provides a higher level of confidence in accuracy since multiple points in the I-V characteristic curve are used. However, this method requires high computational power and a large data memory. The accuracy of the theoretical parameters also depends on the fitting algorithm and criteria. Further, the curve fitting method requires experimental data from the I-V characteristic curve from the manufacturer, which is usually not given in the datasheet.

The PV module contains parasitic resistance which consists of the series resistor, R_s, and the parallel resistor, R_p [87]. The series resistance represents power losses due to the current circulation throughout the PV module [47]. The series resistance does not affect the open circuit voltage and only affects the short circuit current. The increase in series resistance results in the decrease of the short circuit current and reduces the slope of the I-V characteristic curve of the PV module in the constant voltage region. A more accurate calculation of the series resistor is obtained using the curve fitting algorithm; however, there is an equation to calculate series resistor based on the selective point as shown in Eq. (4) [77]. The parallel resistor represents the leakage current at the p-n junction. It does not affect the short circuit current and only affects the open circuit voltage. The increase in parallel resistance results in the decrease of the open circuit voltage and the increase in the slope of the I-V characteristic curve of the PV module in the constant current region. If the slope at the short circuit current in the I-V characteristic curve is almost zero, the parallel resistance is assumed as infinity [77].

$$R_s = \frac{V_{mp} + \dfrac{I_{mp}(V_{oc} - V_{mp})}{(I_{sc} - I_{mp})In\left(1 - \dfrac{I_{mp}}{I_{sc}}\right)}}{I_{mp} + \dfrac{I_{mp}^2}{(I_{sc} - I_{mp})In\left(1 - \dfrac{I_{mp}}{I_{sc}}\right)}} \quad (4)$$

The ideality factor is another component considered when using the PV electrical circuit model. It is also known as the diode quality factor or the n-factor. In an ideal condition, the ideality factor is equal to one. However, in practice, this value varies depending on the non-ideality in the junction behavior. The ideality factor varies from one to two depending on the fabrication process used [47,88]. It is close to one when the diode is dominated by the recombination in the quasi-neutral region and it is close to two when the PV module is dominated by the recombination in the depletion region. Table 1 shows the list of the ideality factor depending on the technology used to manufacture the PV module. However, the ideality factor is different if the curve fitting algorithm is used.

3.1.1.4. Environment factor. The PV panel manufacturer commonly provides the parameter at the Standard Test Condition (STC) where the solar irradiance at STC, G_{ref}, is 1000 W/m^2 and temperature at STC, T_{ref}, is 298 K or 25 °C. For nominal operating cell temperature, NOCT

Table 1
List of ideality factor depending on the PV technology [88].

Technology	Ideality factor
Monocrystalline silicon	1.2
Polycrystalline silicon	1.3
Hybrid amorphous silicon	1.8
Cadmium telluride	1.5

(K), the parameter is determined at an irradiance of 800 W/m^2 and temperature of 20 °C [56]. The parameter extraction only produces the constant value of photo-generated current at a given V_{oc}, I_{sc}, V_{mp} and I_{mp}. This value is manipulated according to solar irradiances and the temperature of the PV module. The PV module temperature affects the I-V PV characteristics. As the temperature increases, the short circuit current increases, open circuit voltage decreases, and maximum power decreases [77,89].

The photo-generated current, I_{ph}, is directly proportional to the sun's irradiance, G (W/m^2) [47,59]. The relationship between I_{ph} and G is shown in Eq. (5) [13,26,48,86,90–94].

$$I_{ph}(G, T) = \frac{G}{G_{ref}}[I_{ph(ref)} + K_{Ti}(T - T_{ref})] \quad (5)$$

where $I_{ph(ref)}$ is the photo-generated current at the STC, K_{Ti} is the temperature coefficient of the short circuit current (A/°C), which is commonly provided by the manufacturer [56], T is the temperature of the PV module (°C), and T_{ref} is the module temperature at the STC.

The saturation current, I_s, is also affected by the environment. However, I_s is only affected by the module temperature and it is not affected by the irradiance. I_s is calculated using Eq. (6) [93,95]. However, a more simplified saturation current equation is used in the PV emulator application [11,26,55,90].

$$I_s(T) = I_{s(ref)}\left(\frac{T}{T_{ref}}\right)^3 exp\left[\frac{qE_g}{Ak}\left(\frac{1}{T_{ref}} - \frac{1}{T}\right)\right] \quad (6)$$

where $I_{s(ref)}$ is the saturation current at the STC, q is electron charge (1.6×10^{-19} C), k is Boltzmann's constant (1.38×10^{-13} J/K), and E_g is the thermal gap (eV).

There are also other terms called the thermal voltage, V_T, and the thermal gap which are affected by the environment in the PV electrical circuit model. The thermal voltage increases as the temperature increases and it this is represented in Eq. (7) [47,51,96]. The thermal gap, E_g is 1.12 eV for the crystalline silicon PV panel and 1.75 eV for the amorphous silicon PV panel [79].

$$V_T = \frac{kT}{q} \quad (7)$$

3.1.2. Interpolation model
The PV interpolation model is another type of PV model capable of producing the I-V characteristic curve of the PV module. This model is a mathematical function that intercepts the short circuit current, I_{sc} and open circuit voltage, V_{oc}. There are various types of interpolation models used in the PV emulator [20,45,50,84,97]. These models have PV voltage, V_{pv} as the input and PV current, I_{pv} as the output as shown in Table 2 and are capable of producing the I-V characteristic curve of PV at different irradiance, G and temperature, T.

The interpolation model requires specific points on the I-V characteristic curve. The common points required are the I_{sc} and V_{oc} at STC [20,45,84]. However, some models require the I_{sc} and V_{oc} at other irradiance and temperature levels, as shown in Table 2. These points are open circuit voltage at 1000 W/m^2 0 °C ($V_{ocG1000T0}$) [97], short circuit current at 1000 W/m^2 0 °C ($I_{scG1000T0}$) [97], and open circuit voltage at 200 W/m^2 25 °C ($V_{ocG200T25}$) [45]. The manufacturer commonly provides the I_{sc} and V_{oc} at STC only. Therefore, the additional requirement reduces the flexibility of the interpolation model.

Besides I_{sc} and V_{oc}, the maximum power voltage and current (V_{mp} and I_{mp}, respectively) is required for a part of the interpolation model [84]. The interpolation model sometimes requires the series resistance, R_s, as shown in Table 2. The module temperature, T also affects the I-V characteristic curve produced. The temperature effect is presented as the constant temperature coefficient of the open circuit voltage and

Table 2
The interpolation model used in the PV emulator application.

Reference	Khouzam and Hoffman [84]	Garai [97]	Xenophontos et al. [45]	Gonzalez-Llorente et al. [20]	Lee et al. [50]
Model input	V_{pv}, G, T	V_{pv}, G, T	V_{pv}, G, T	V_{pv}, G, T	V_{pv}, G, T
Model output	I_{pv}	I_{pv}	I_{pv}	I_{pv}	I_{pv}
STC parameter	V_{oc}, I_{sc}, V_{mp}, I_{mp}	(not used)	V_{oc}, I_{sc}	V_{oc}, I_{sc}	V_{oc}, I_{sc}
Temperature coefficient	K_{ti}, K_{tv}	K_{ti}, K_{tv}	K_{ti}, K_{tv}	K_{ti}, K_{tv}	(not used)
Additional requirement	R_s	$V_{ocG1000T0}$, $I_{scG1000T0}$	$V_{ocG200T25}$	(not used)	$V_{ocG200T25}$, $I_{scG200T25}$, $V_{ocG1000T0}$, $I_{scG1000T0}$, $V_{ocG1000T0}$, $I_{scG1000T0}$, (not used)
Adjusting parameter	(not used)	b	b	b	

short circuit current (K_{tv} (V/°C) and K_{ti} (I/°C), respectively). K_{tv} and K_{ti} are commonly provided by the manufacturer. One of the PV interpolation models requires the minimum and maximum irradiance and temperature points of the I_{sc} and V_{oc} [50]. This method does not take advantage of the K_{tv} and K_{ti} provided by the manufacturer. However, the irradiance coefficient is derived since it is rarely provided by the manufacturer. The characteristic constant, b is present in the interpolation model as shown in Table 2 [20,45,97]. b is adjusted until the I-V characteristic curve produced by the model follows the I-V characteristic curve produced by the actual PV panel.

3.1.3. Discussions on type of photovoltaic models

The PV electrical circuit model and the PV interpolation are based on different concepts. The PV electrical circuit model is derived based on the electrical characteristics of the PV module. However, the PV interpolation model is derived from the I-V characteristic curve of the PV module. The PV electrical circuit model contains the implicit equation which requires a numerical method such as the Newton-Raphson method to obtain a solution [45,58,70–72,90,98,99]. In fact, the numerical method requires multiple calculations of the same equation to obtain a converged solution. Therefore, the calculation time is longer for the electrical circuit model compared to the interpolation model. The interpolation model is faster than the electrical circuit model because there is no implicit equation inside the model as shown in Table 3. Therefore, the interpolation model requires only a single calculation to obtain the convergence solution.

The electrical circuit model also requires theoretical parameters such as the ideality factor, series resistance, and parallel resistance for the model to work. These theoretical parameters are obtained through a process called the parameter extraction. The parameter extraction involves the complex mathematical equation and a high processing power. However, this complex process is not commonly implemented into the PV emulator controller and is done offline (not during emulation process). The parameter extraction process is not required in the interpolation model, as shown in Table 3. However, the interpolation model requires the short circuit current and the open circuit voltage at conditions other than the STC. This point is not commonly provided by the manufacturer. Further, the interpolation model has an adjusting parameter which has no specific ways to be calculated and requires the trial-and-error method to determine its

parameters. Since the PV electrical circuit model represents the actual electrical characteristic of the PV module, this model has a higher accuracy compared to the PV interpolation model.

The electrical circuit model used in designing the PV emulator varied with each researcher. The commonly used electrical circuit model is the 1D1R model [18,25,39,73–76] and 1D2R model [17,42,50,100]. This is due to its simplicity and the accurate representation of I-V characteristic of these models.

The single diode model is suitable for the PV module with the amorphous silicon construction (usually using thick-film deposition technique) [63] and for a high power PV generation since the irradiance used in the simulation is usually high [47]. Since the PV module that used the amorphous silicon construction does not show the same sharp knee characteristic as the crystalline type, the saturation current due to the diffusion mechanism is set to zero as shown in Eq. (1) [47,63]. Therefore, this model is not suitable for PV cell with polycrystalline silicon construction [63]. It is also not suitable for simulating low irradiance conditions since the model does not consider the space charge recombination effects [47,96].

The double diode model is a more accurate representation of the PV module compared to the single diode under low solar irradiance conditions [65]. The double diode model is more suitable for simulating the partial shading conditions due to its accuracy under low irradiance conditions [57]. This model is also suitable for the monocrystalline silicon or the polycrystalline silicon type of PV module [47,63,65]. However, it is a more complex model since more parameters are considered, which requires more computational time compared to the single diode model [25,57].

Since the PV emulator focuses on a large power application that requires a high-level solar irradiance, the 1D2R model is enough for the PV emulation application. For the 1D1R model, the absence of a parallel resistor does not highly affect the constant current region and only affects the constant voltage region [47,83]. Since the operation of the PV emulator is commonly in between the constant current region and the constant voltage region (the PV emulator is commonly connected to the MPPT device which operates between these regions), the absence of a parallel resistor does not significantly affect the accuracy of the model. Therefore, the suitable PV model for the PV emulator is the 1D2R model and the 1D1R model.

3.2. Implementation of photovoltaic model

The PV mathematical model is implemented into the controller to calculate the reference signal for the PV emulator. However, the complex mathematical equation burdens the processor of the controller. As a result, the calculation of the reference point for the PV emulator is delayed which results in incorrect responses to disturbances. This shows the importance of the PV model calculation in real-time for the PV emulator. Therefore, a suitable implementation method is needed depending on the capability of the controller and the complexity of the PV model. There are five methods used to implement the PV model into the PV emulator controller as shown in Fig. 2.

Table 3
Comparison between the electrical circuit model and the interpolation method.

Parameter	Electrical circuit model	Interpolation model
Implicit equation	Present	Absent
Numerical solution	Required	Not required
Convergence time	Slower than the interpolation model	Faster than the electrical circuit model.
Theoretical parameter	Required through parameter extraction	Not commonly required
Accuracy	Higher than the interpolation model	Lower than the electrical circuit model

3.2.1. Direct calculation method

The direct calculation method is implementing the PV model directly into the PV emulator controller. The commonly used PV model for this method is the 1D1R model [12,19,25,26,39,72,73,81]. This is because the 1D1R model is less complex compared to the 1D2R model and 2D2R model, and more accurate than the 1D model. However, the 1D model [27] and 1D2R model [11] are also implemented using this method.

The 1D1R model requires the theoretical parameter to generate the I-V characteristic curve. This parameter is either extracted using the parameter extraction process [11], obtained from the datasheet [73], or used the curve fitting process [39]. The 1D1R model used in the direct calculation method is sometimes simplified to reduce the processing burden of the controller. The complexity of the 1D1R model is due to the diode current equation. This equation is modified and a simpler equation is derived [12,25]. This simplified model only requires a selective point from the I-V characteristic curve of PV and temperature coefficient of the open circuit voltage. Besides modifying the diode current equation, there is also another method used to simplify this equation. The reverse saturation current of the diode is a part of the diode current equation. The original equation of the reverse saturation current is highly complex [11]. However, the complexity is reduced if the temperature coefficient of the short circuit current and open circuit voltage are available [26].

3.2.2. Look-up table method

The look-up table (LUT) method is one of the more commonly used methods in the PV emulator application [13,30,31,33,43,68,101–103]. There are several types of look-up table methods used to represent the I-V characteristic of the PV module. The basic type is the I-V or the V-I look-up table, as shown in Table 4. The I-V look-up table has the PV voltage, V_{pv}, as the input of the table and PV current, I_{pv}, as the output of the table. While the V-I look-up table has I_{pv} as the input of the table and V_{pv} as the output of the table. The output of the look-up table usually becomes the reference signal for the closed-loop converter system of the PV emulator. There is an improved control strategy of the PV emulator that uses both the I-V and V-I look-up table, as shown in Table 4 [14].

In addition to the I-V and V-I look-up table, the input and the output of the table are modified to overcome the limitations of the basic look-up table. The V-R look-up table (PV resistance, R_{pv}, as the input of the table and V_{pv} as the output of the table) offers more stable reference signal since the table input produced by dividing the output current and the output voltage are not affected by the output ripple. The R_{pv} array inside the look-up table is determined by dividing V_{pv} over the I_{pv} [44,101,102]. There is also the V & I − R look-up table (R_{pv} as the

input of the table, V_{pv} and I_{pv} as the output of the table) that provides the voltage and current reference signal based on the output resistance [13]. The P-V look-up table is used to overcome the compatibility problem with the MPPT-based PV inverter [103]. There is also a look-up method that does not depend on V_{pv} and I_{pv}. The look-up table stores the I-V characteristics of the diode represented inside the electrical circuit model [68]. Since the diode is not affected by the irradiance, the dynamic irradiance manipulation is done without the need of a large sampling point of the I-V characteristic curve at different irradiance. However, the change in temperature requires the reloading of the diode I-V characteristic data [68].

3.2.3. Piecewise linear method

The piecewise linear photovoltaic model is the curve fitting process using multiple segmented straight lines which follow the I-V characteristic curve of the PV module. This method commonly consists of two linear lines and is the minimum number of lines applied in the PV emulator system [34,36,104]. However, a higher number of linear lines increases the accuracy of the PV model used for the PV emulator application [35,37].

There are two approaches to derive the equation for the piecewise linear PV model. The first approach is to use the selective point of the PV module. The selective point consists of the I_{sc}, V_{oc}, and maximum power point (I_{mp} and V_{mp}) which are available in the manufacturer datasheet of the PV module. Since the manufacturer only gives these three points at the STC, this type of PV model is only capable of generating the I-V characteristic curve at the 1000 W/m² and 25 ℃ [34,36]. However, this method is improved by introducing the functions that manipulate the three selective points according to the irradiance and module temperature [35]. Besides the limitation of changing irradiance and temperature, this model is only capable of generating two linear lines since the available point is three. The first line is from the I_{sc} to maximum power point and the second line is from maximum power point to V_{oc} [34,36]. This limitation can be overcome by adding two more linear lines to fit the I-V characteristic curve [35]. This is done by introducing two more additional points 5% before and after the maximum power point.

The second approach is to plot the straight line directly on the I-V characteristic of the PV curve. In the PV emulator application, the minimum numbers of straight lines used for this approach is two [34], while the maximum number of straight lines used for this approach is five [37]. The slope and the y-axis intersection of each line drawn are determined graphically. For this approach, there is no limitation on the number of the lines used to fit the I-V characteristic curve. However, the irradiance and module temperature could not be manipulated during the PV emulator operation.

Table 4
The type of look-up table implemented in the PV emulator control system.

LUT type (Output-input)	Data source	Online G and T change	Controller	Point	Reference
Basic look-up table					
I-V	Ideal PV model	Not capable	FPGA	255	Koutroulis et al. [5]
	Experiment data	G	Microcontroller	26	González-Medina et al. [56]
	1D2R model	Not capable	DSP	1000	Zhao and Kimball [99]
	1D2R model	n/a	DSP	1000	Weichao and Kimball [29]
V-I	Experiment data	Not specified	Microcontroller	Not specified	Qingrong et al. [23]
	Manufacturer datasheet	G and T (3 discrete curve)	DSP	Not specified	Gadelovits et al. [64]
	Not specified	G and T	Microcontroller	Not specified	Barrera et al. [30]
I-V & V-I	1D2R Model	G (Not specified)	Microcontroller	1024 & 4096	Kim et al. [29]
Modified look-up table					
I_d-V_d	PV model (Not specified)	G	FPAA	256	Barra et al. [68]
P-V	Not specified	Not specified	FPGA	4096	Chavarría et al. [61]
	Not specified	Not specified	No Hardware	Not specified	Chavarría et al. [94]
V-R	Experiment data	Not specified	FPGA	Not specified	Iqbal et al. [32]
	PV model (Not specified)	G (2 discrete curve)	Computer with LabVIEW platform	Not specified	Bhise et al. [25]
I & V - R	1D model	G & T	DSP	Not specified	Kim et al. [13]

3.2.4. Neural network method

The implementation of the neural network PV model in the PV emulator is uncommon [12,38]. In general, I-V characteristic data is obtained either from the experimental process [38] or the electrical circuit PV model [12] at different loads, irradiance, and temperature. The data is trained offline before the neuron network PV model is generated. The training process generates the PV hyper-surface in the current-voltage-irradiance-temperature working space. Since the working space is four dimensions, the number of neurons is carefully chosen. After the training process is completed, the neural network PV model is implemented inside the PV emulator controller.

The growing neural gas (GNG) network is used in implementing the neural network PV model [12]. The GNG allows new neurons to grow from the initially small networks. The advantages of the GNG is the lower computational burden compared to the classic multilayer perceptron trained by the back-propagation algorithm.

3.2.5. Photovoltaic voltage elimination method

The photovoltaic voltage elimination method used two different PV characteristic equations to produce a single I-V characteristic curve. This curve is separated into two regions by the critical load line [40] to reduce the burden of the PV emulator controller. In the constant current region, the PV voltage is assumed as zero since the change in PV voltage does not significantly affect the PV current. The constant current region and the constant voltage region are separated by the critical load lines. The critical load lines intersect on the I-V characteristic curve which is located at a point 99% of the short circuit current. The PV voltage is considered into the PV mathematical model when the PV current is less than or equal to 99%. However, this method only reduces the processing burden if the PV emulator operating point is located in the constant current region.

3.2.6. Discussions on implementation of photovoltaic models

The direct calculation method is the unmodified PV model implemented into the PV emulator. Since the calculation of the PV model is done in real-time, the controller of the PV emulator suffers from high processing burdens, as shown in Table 5. The 1D1R model is commonly used in the direct calculation method [11,12,19,25,26,72,73]. This model contains implicit equations that requires the numerical method such as the Newton-Raphson method to solve the equation [45,58,70–72,90,98]. Therefore, the mathematical equation of the 1D1R model is calculated multiple times before a solution is converged. When the 1D1R model is calculated multiple times before the solution is obtained, the process of finding the operating point for the PV emulator is delayed. This affects the dynamic performance of the PV emulator especially if the MPPT device or power conditioning system is connected to the PV emulator.

The memory requirement for the direct calculation method is lower compared to the look-up table method. The accuracy of the PV model implemented inside the controller is an important aspect of the PV emulator application. For the look-up table method and the piecewise linear method, the I-V characteristic curve is in the discrete form. If the operating point of the PV emulator is between these discrete points, the interpolation process is done between these points. Therefore, the operating point produced from the interpolation process is inaccurate since the point produced by the look-up table method or the piecewise linear method is only the estimation between two points. If the distance between these two points is far apart, the estimated operating point becomes inaccurate. Since there is no modification done toward the PV model when using the direct calculation method, the accuracy of the PV model is not compromised.

An advantage of the look-up table method is the reduction in the processing burden, as shown in Table 5. Besides, this method allows the use of the I-V characteristic data of the PV obtained from the experiment. Therefore, the parameter extraction process used in determining the theoretical parameter of the PV module is avoided. However, this method requires a large memory storage from the controller to allow an accurate emulation of the PV. A smaller memory capacity is needed if a small number of sampling points of the I-V characteristic curve is used. However, the small sampling point reduced the accuracy of the PV model. As a result, the accuracy of the PV emulator is reduced. A large number of sampling points increases the accuracy of the PV module. However, storing the sampling point data is limited to the capability of the hardware platform. The adaptability of the look-up table is also low since a new set of I-V characteristic data is needed when a different type of PV panel is emulated.

The piecewise linear photovoltaic model is a simple PV model which consists of multiple linear lines. The simplicity of this model allows a low computational and a low-cost controller to be used in the PV emulator [37]. As a result, a higher switching frequency can be implemented and this reduces the size of the LC filter. A small LC filter improves the dynamic performance of the PV emulator. However, the piecewise linear PV model suffers from a low accuracy output, as shown in Table 5. This is because the piecewise linear PV model that uses the selective point is only capable of producing two straight lines [34,36]. However, the piecewise linear PV model using the graphical method is able to produce a higher number of straight lines and increases the accuracy of the PV model [37]. Even though the accuracy is improved by increasing the number of linear lines, the adaptability of this model is low since the graphical method requires the complete I-V characteristic curve rather that the three selective points provided by the manufacturer. Therefore, the new piecewise linear function is derived when the different PV model is emulated. Besides flexibility and accuracy problems, the piecewise linear photovoltaic model is unable to change the irradiance and temperature when the PV emulator is operating. This problem is overcome by introducing the selective point function according to the irradiance and the module temperature.

The neural network method requires offline training of the I-V

Table 5
The comparison of the PV model implementation method.

Parameter	Direct calculation method	Look-up table method	Piecewise linear method	Neural network method	Photovoltaic voltage elimination method
Processing burden	High burden	Low burden	Low burden	Depends on the number of neurons used	High burden (lower in the constant current region)
Memory array used	Low memory usage	High memory usage	Low memory usage	Depends on the number of neurons used	Low memory usage
Accuracy	High accuracy	Accurate (depends on the number of points)	Low accuracy	Accurate	High accuracy
Adaptability[a]	Depends on the model used	Low flexibility	Depends on the model used	Low flexibility	Depends on the model used
Online GT setting	Capable	In discrete form	Generally incapable	Capable	Capable

[a] Adaptability is the flexibility of the PV model implementation method to change the I-V characteristic curve when the different type of PV panel is emulated.

characteristic data. Therefore, the adaptability of this model is low since the new training process is required when a different type of PV panel is emulated. However, this method has the ability to change the irradiance and temperature during the PV emulator operation. The PV voltage elimination method is similar to the direct calculation method. However, the burden is slightly reduced when the PV emulator operates in the constant current region.

4. Control strategy

The function of the control strategy of the PV emulator is to determine the operating point of the PV emulator. It locates voltage and current on the I-V characteristic curve of the PV module corresponding to the output resistance. This is different from the MPPT algorithm since the aim of the MPPT algorithm is to find the highest point of the power-voltage (P-V) characteristic curve of the PV module. Even though the control strategy of the PV emulator is the crucial part of the PV emulator control system, it is rarely being improved. Fig. 6 shows the control strategy implemented for the PV emulator control system which consists of the type of control strategy, partial shading implementation, and methods of implementing the controller in the PV emulator application.

4.1. Type of control strategy

4.1.1. Direct referencing method
The basic control strategy implemented for the PV emulator is the direct referencing method. It is a common control strategy used in the PV emulator control system since it does not require an additional algorithm to determine the operating point of the PV emulator [7–12,25,26,34,36,48,66,68,87,104,105]. The direct referencing method is not specified to the switched-mode power supply (SMPS) only. This control strategy is also being used with the linear regulator [82]. However, it is more commonly found in the PV emulator using the SMPS.

This method is categorized into two types depending on the closed-loop system and the PV model used for the PV emulator. The current-mode controlled system requires the PV model with the PV module voltage, V_{pv}, as their input ($I = f(V)$), as shown in Fig. 7 [7–11,48,55,68]. The output voltage, V_o, of the PV emulator is connected to the PV model input. At the
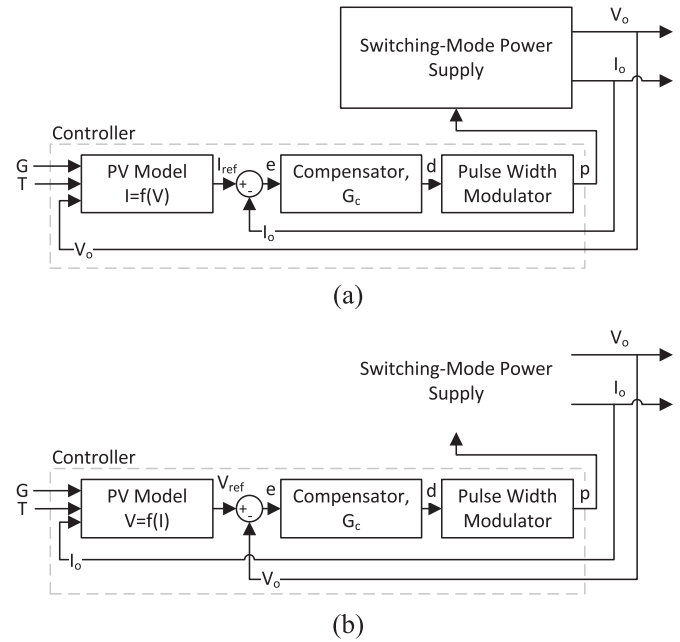
(a)

(b)

Fig. 7. The direct referencing method for the PV emulator using the a) current-mode controlled switching-mode power supply system with the V_o as the PV model input b) voltage-mode controlled switching-mode power supply system with the I_o as the PV model input.

beginning, the V_o is equal to zero and the PV model produced the reference current signal, I_{ref}, equal to the short circuit current of the PV model, I_{sc}, at the given irradiance, G and PV module temperature, T. As V_o increases, I_{ref} begins to decrease following the I-V characteristic curve of the PV module. The PV emulator reaches a stable operating point when V_o and the output current, I_o, correspond to the output resistance, R_o, on the I-V characteristic curve.

The voltage-mode controlled system requires the PV module current, I_{pv}, to be the PV model input ($V = f(I)$) [12,25,26,34,36, 66,81,87,104,105]. The I_o of the PV emulator is connected to the PV model input. At the beginning, I_o is equal to zero and the PV model produced the reference voltage signal, V_{ref}, equal to the open circuit
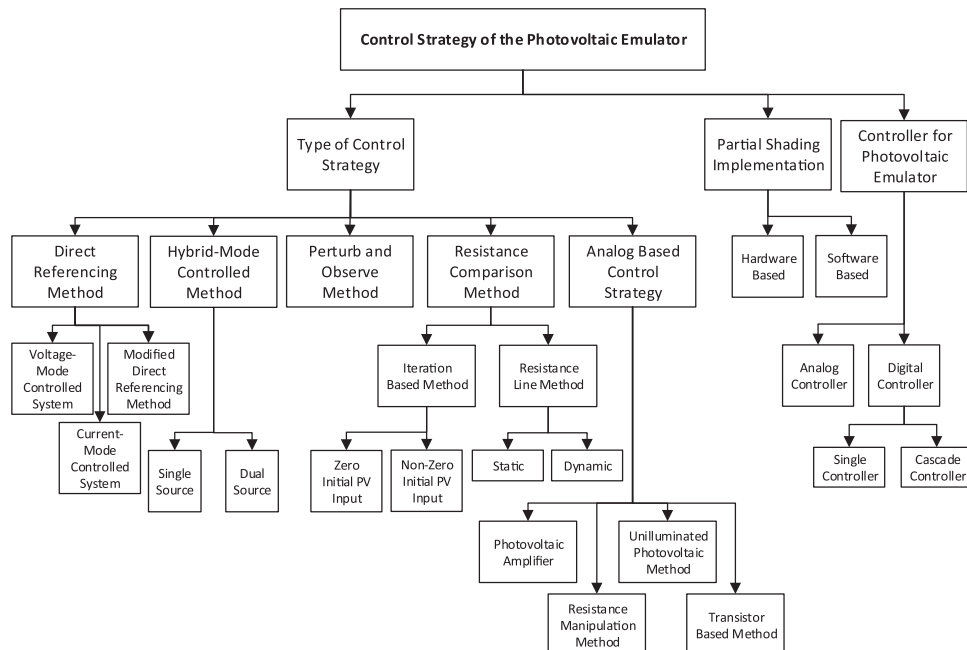
Fig. 6. The control strategy of the PV emulator.

voltage of the PV model, V_{oc}, at given G and T. As I_o increases, V_{ref} begins to decrease following the I-V characteristic curve of the PV module. A stable operation of the PV emulator is achieved when the V_o and the I_o is on the point of the I-V characteristic curve of the PV module corresponding to the R_o.

The common direct referencing method uses the dynamic characteristic of the closed-loop converter system to solve the operating point of the PV emulator. However, there is also a method that used the iteration process to determine the operating point [106]. The method is called 'the two algorithm' and it is implemented using the LabVIEW platform. This method used the difference between the output of the PV emulator and the PV model to determine the step size of the iteration. The voltage and current difference are continuously checked and the new operating point is calculated if the difference is large. The performance of the direct referencing method is improved by using an adaptive PI controller [107]. The PI controller is trained using the artificial neural network at different loads and irradiance. As a result, the transient response and the stability of the PV emulator are maintained for various conditions.

4.1.2. Hybrid-mode controlled method

The PV module has nonlinear characteristics. In the constant current region, the V_{pv} varies significantly and the I_{pv} is almost constant; and vice versa in the constant voltage region. The conventional closed-loop converter system has a constant reference point. However, the reference point for the PV emulator is varied due to the nonlinear characteristics of the PV module. Variation in the reference point affects the stability of the closed-loop of the converter system. As a result, the output of the PV emulator oscillates [13,14].

The stability of the PV emulator is improved by implementing the different direct referencing method according to the region of the I-V characteristic curve of the PV module. This implementation method is called the hybrid-mode controlled method. When the operation of the PV emulator is in the constant current region, the I_{pv} is almost constant. Therefore, the PV emulator in the constant current region needs to operate in the current-mode controlled system. While, when the operation of the PV emulator is in the constant voltage region, the V_{pv} produced is almost constant. Therefore, the PV emulator in the constant voltage region is operated in the voltage-mode controlled system.

There are two ways to implement the hybrid-mode controlled method., by either using the single source [14,15] or the dual source [13]. The single source hybrid-mode controlled method used only a single power converter, while the dual source hybrid-mode controlled method used two power converters which consist of a voltage source and a current source.

The PV emulator uses a single source and the hybrid-mode controlled method uses the SMPS [14]. The converter is controlled using the PI controller. This PV emulator used three look-up tables which consist of an I-V table, V-R table, and V-I table. The I-V characteristic curve of the PV module is divided by two resistance points (R_I and R_V, where $R_I < R_V$) obtained through the analytical process. As a result, the I-V characteristic curve is divided into three parts. The first part is the constant current region and the algorithm used the I-V table to obtain the reference current for the PV emulator. The PV emulator operates in this region when the output resistance is below R_I. At this region, the PV emulator is in the current-mode controlled operation. If the output resistance is more than the R_I, the PV emulator is in the voltage-mode controlled operation. At the region between R_I and R_V, the voltage and current are not constant. To avoid the issue of oscillation, the V-R table is used to produce a stable reference voltage for the PV emulator. If the output resistance is more than the R_v, the V-I table is used. To avoid unstable switching between operation modes, the area between the switching operations is overlapped.

The linear voltage and current regulator are used in the dual source

hybrid-mode controlled method [13]. Both linear regulators are controlled using two separate PID controllers. The two linear regulators are connected in parallel with the load. A diode is added in series at each linear regulator to allow a smooth transition between the current regulator and the voltage regulator. The region between the current regulator operation and voltage regulator operation is overlapped to avoid unstable switching between the two sources. This method is called hysteresis switching and it requires two voltage points (V_1 and V_2 which $V_1 < V_2$). When the PV emulator operates as the current source and the output resistance increased, the PV emulator operates as the voltage source when the output voltage is more than the V_2. When the PV emulator operates as the voltage source and the output resistance decreased, the PV emulator operates as the current source when the output voltage is more than the V_1.

In conclusion, the hybrid-mode controlled method is able to eliminate the instability problem faced by the direct referencing method. However, this control strategy is very complex. If the dual source is used, the cost is increased since the two power converters are used. Besides, the hybrid-mode controlled method requires more than two separate look-up tables to operate which requires a large storage memory.

4.1.3. Hill climbing method

The hill climbing (HC) method and the perturb and observe (P & O) method are also used in the PV emulator control strategy, as shown in Fig. 8(a) and (c) [19,20,108]. Unlike the direct referencing method, the hill climbing method and the perturb and observe method use a fixed step size which produces a more stable output.

The hill climbing method is simpler compared to the perturb and observe method since no compensator is used in the control strategy. Therefore, the processing burden only focused on the PV model. The hill climbing method is based on the simple algorithm as shown in Fig. 8(a) and (b) [19,20]. When the PV emulator starts, V_o and I_o are measured and the signal is transferred to the controller. The I_{pv} is calculated based on V_o, irradiance (G), and temperature (T). The I_{pv} is then compared with I_o. If I_{pv} is larger than I_o, I_o increases. To increase I_o, V_o is increased by augmenting the duty cycle, D. The duty cycle is increased according to the constant duty cycle step size, D_{step}. However, if I_{pv} is smaller than I_o, I_o decreases. To decrease I_o, V_o is decreased by reducing the duty cycle. The duty cycle is decreased according to the constant D_{step}. Even though this method is simple, the PV emulator suffers slow dynamic responses or oscillates outputs due to the constant D_{step}.

The perturb and observe method uses a PI controller instead of increasing the duty cycle directly, as shown in Fig. 8(c) [108]. The duty cycle changes are replaced with the reference current changes, I_{ref}, as shown in Fig. 8(d). The I_{pv} is calculated based on V_o, G, and T. The perturb and observe method compares the I_{pv} with I_o. If I_{pv} is larger than I_o, the reference input, I_{ref}, is decreased by subtracting I_{pv} with the current step size, I_{step}, while if I_{pv} is smaller than I_o, I_{ref} is increased by adding I_{pv} with I_{step}.

4.1.4. Resistance comparison method

The resistance comparison method is another type of control strategy for the PV emulator. The PV model is either V as the input with I as the output ($I = f(V)$) or I as the input with V as the output ($V = f(I)$). Therefore, the PV model is modified in order to receive resistance, R as the input ($[V, I] = f(R)$). R_o is produced digitally inside the controller by dividing V_o over I_o, as shown in Fig. 9. The resistance comparison method is used in the current-mode [17,18] or voltage-mode [16,97] controlled SMPS system. Besides the SMPS, the resistance comparison method is also used in the programmable power supply [40,70,72,102]. The programmable power supply enables the current-mode and the voltage-mode controlled operation. Since the resistance comparison method is capable of producing I_{ref} and V_{ref} simultaneously, this method is suitable for the PV emulator using the
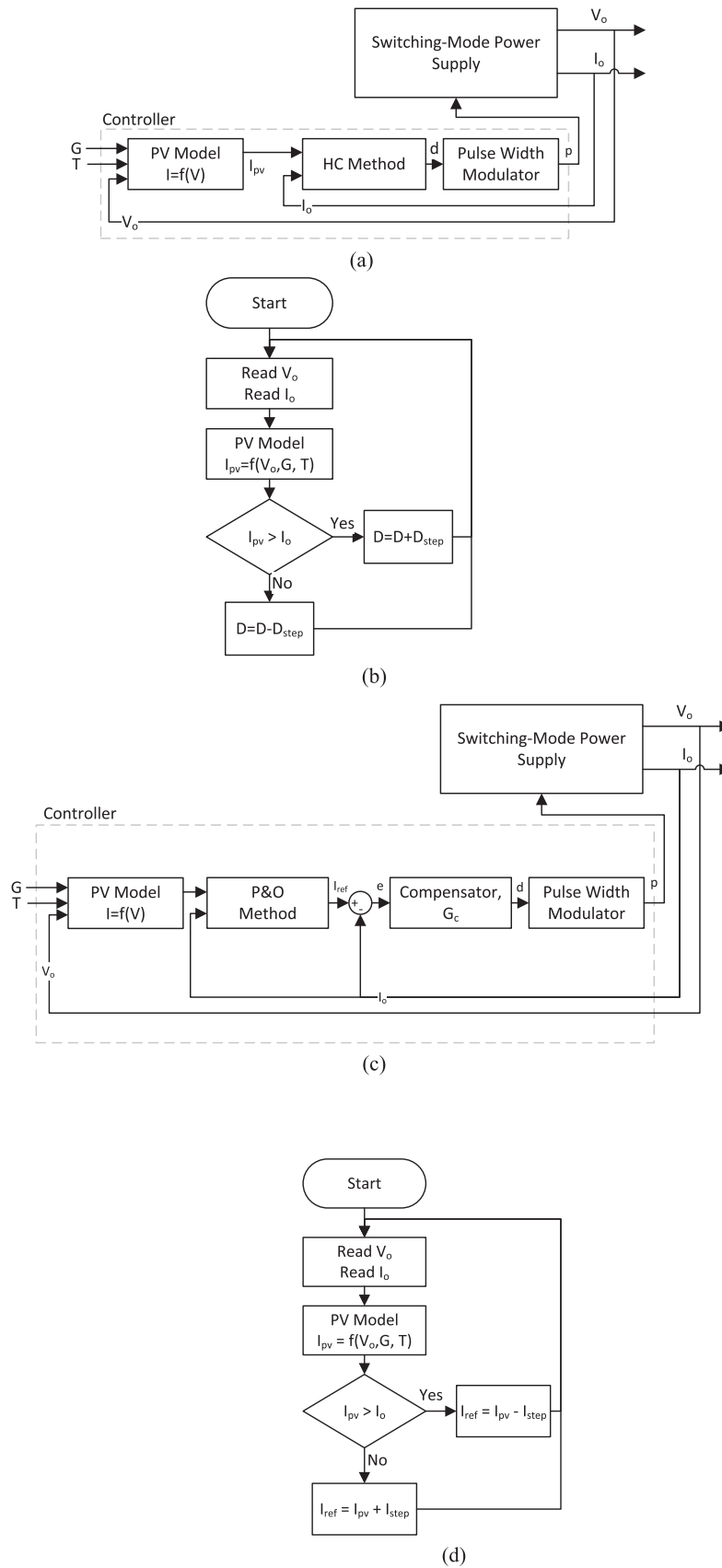
Fig. 8. (a) The block diagram and (b) the control algorithm of the hill climbing method for the PV emulator. (c) The block diagram and (d) the control algorithm of the perturb and observe method for the PV emulator.
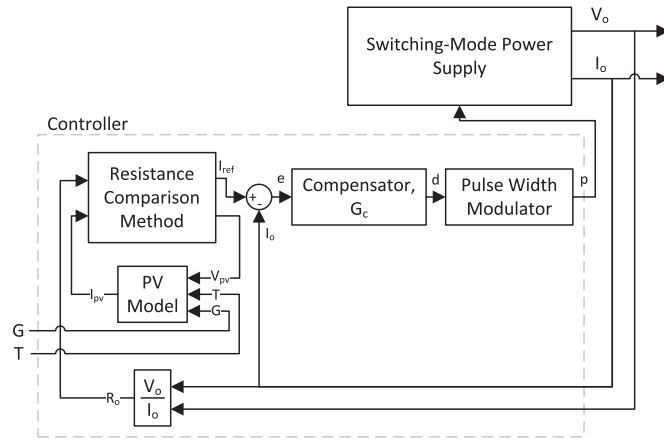
Fig. 9. The resistance comparison method for the PV emulator using the current-mode controlled switching-mode power supply system.

programmable power supply [45,102].

The resistance comparison method is divided into two categories, namely the iteration based method and the resistance line method. The basic principal of the resistance comparison method is comparing the R_o obtained by dividing the V_o over the I_o with the PV module resistance, R_{pv}, by dividing the V_{pv} over the I_{pv}.

4.1.4.1. Iteration based method. The iteration based method is one of the resistance comparison methods. The PV model used is either V_{pv} or I_{pv} as the input. This input is called the PV model input. The iteration based method is categorized into two types depending on the initial PV model input. The first type is the zero initial PV model input [16,17] and the second type is the non-zero initial PV model input [18], as shown in Fig. 10.

The zero initial PV model input starts the iteration process from zero V_{pv} for PV model with V_{pv} as the input and zero I_{pv} for the PV model with I_{pv} as the input [16,17]. The V_{pv} increases at a constant step size until V_{pv} equals to V_{oc} and R_{pv} is calculated at each iteration [17]. After the first iteration is completed, the second iteration is done to determine I_{ref} by comparing the R_o with R_{pv}. This method requires a full sweep of the I-V characteristic curve of the PV module at the beginning of the iteration or when G and T changed. Therefore, this method is not suitable for the PV emulator with the dynamic change of G and T. Another method is to simultaneously calculate R_{pv} and compare R_{pv} with R_o [16]. The iteration process started from zero I_{pv} and increased with a constant step size. The V_{ref} is determined when R_{pv} is equal to or smaller than R_o, as shown in Fig. 10. This method is capable of handling dynamic changes in G and T; however, it requires a high number of iterations to determine the operating point of the PV emulator.
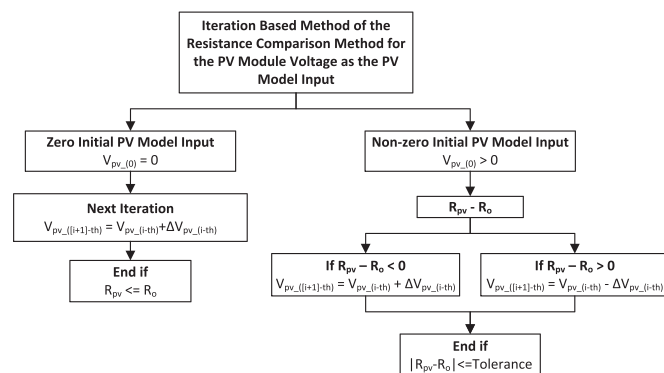
The calculation for the non-zero initial PV model input is more complex than the zero initial PV model input [18]. The iteration process started with V_{pv} equal to V_o. The V_{pv} increases from V_{oc} with a fixed step size, and R_{pv} is calculated for every iteration. There are two conditions verified for every iteration. The first condition is the error of the resistance. The error of resistance is the difference between R_{pv} and R_o. I_{ref} is produced if the error of the resistor is below the tolerance value. The second condition is the increasing or the decreasing decision of V_{pv}. The range of R_{pv} is small when the point is near I_{sc} and large when the point is near V_{oc} on the I-V characteristic curve. If R_{pv} is smaller than R_o, V_{pv} increases. While, if R_{pv} is larger than R_o, V_{pv} decreases, as shown in Fig. 10.

4.1.4.2. Resistance line method. The resistance line method is one of the resistance comparison methods that use the graphical construction process instead of mathematically analyzing the location of the R_o on the I-V characteristic curve of the PV module [32,45,98,101,102]. The I-V PV data at a given G and T is collected from the PV model. This data is plotted with the inverse output resistance line and the interception between these two lines is the operating point of the PV emulator, as shown in Fig. 11.

There are two types of the resistance line method implemented in the PV emulator. The first type is the static resistance line method [101,102]. This type of resistance line method only stores the I-V data at a given G and T. Another set of I-V data is loaded into the controller for the different G and T. Therefore, this method is not suitable for testing the dynamic G and T conditions. The second type is the dynamic resistance line method [32,45,98]. This method includes the PV model in the resistance line method. When there is a change in G and T, the PV model is swept to obtain the I-V data. However, the change in the G and the T is required in the form of a step change. The gradual change of the G and the T requires a constant sweeping process that burdens the controller.

4.1.5. Analog based method

The direct referencing method and the resistance comparison method is the common control strategy used in the PV emulator. However, there is also another type of control strategy used to emulate the characteristics of the PV module which is the analog based method. The analog based method could not be implemented in the digital form since it depends on the characteristics of the analog circuit.

4.1.5.1. Photovoltaic amplifier method. The early design of the PV emulator is implemented using the PV amplifier [4,21,22,109,110]. A single PV cell is connected to a linear amplifier that consists of the Darlington connection [4]. To ensure the accuracy of the PV emulator,
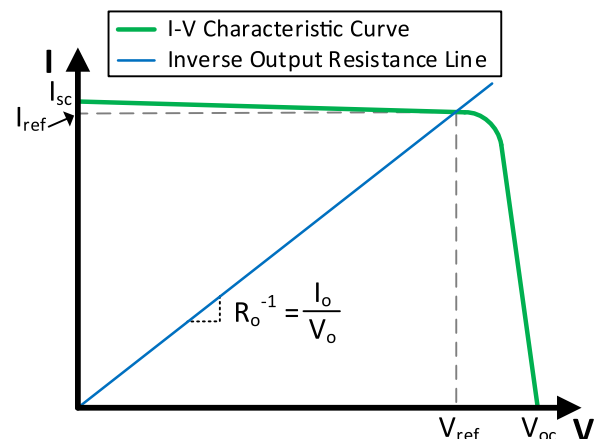

Fig. 10. The iteration based method with the resistance comparing processes in each iteration where the PV model input is the PV module voltage.

Fig. 11. The resistance line method used to determine the reference current, I_{ref} and reference voltage, V_{ref} for the PV emulator.

the system is equipped with the output current feedback loop. The irradiance is emulated using the halogen lamp controlled by using the variable DC voltage supply. However, this method is not flexible since it requires the actual PV cell to emulate the PV panel.

This problem is overcome by replacing the PV cell with the photo-sensor or the photodiode [21,22,109,110]. The various types of PV panel are emulated by adjusting the specific resistor inside the PV emulator [109]. The irradiance exposed to the photo-sensor is controlled using the light from the light emitting diode (LED) connected through the fiber optic. The light intensity produced by the LED is controlled using a computer that is connected through the digital to analog converter (DAC) [109] or the analog PWM generator [21]. The module temperature of the PV panel is also emulated by attaching a small ceramic heater to the photosensor [109].

4.1.5.2. Resistance manipulation method.
The resistance manipulation method is another analog based method for the PV emulator [93,111,112]. This method is simpler compared to other analog based methods used in the PV emulator since it only requires a DC power supply and a variable resistor. The irradiance is controlled by adjusting the current limiter of the DC power supply.

One of the resistance manipulation methods used the maximum power transfer theorem to test the MPPT device and power conditioning system [93,111]. The theorem shows that maximum power is achieved when the series resistance is equivalent to the load resistance, the MPPT device and power conditioning system. Although this PV emulator is simple, the I-V characteristic curve produced by the resistance manipulation method is very different from the PV I-V characteristic curve. The maximum power point voltage of the resistance manipulation method is located at half of the open circuit voltage. The common maximum power point voltage for PV I-V characteristic curve is usually located near to open circuit voltage. Even though the I-V characteristic produced is highly inaccurate, this method is used in testing the MPPT device and power conditioning system if the aim of the test is to investigation the capability of the system to determine the maximum power point.

Another type of resistance manipulation method is the PWM switch resistor [112]. The I-V characteristic curve produced using this method is more accurate compared to the resistance manipulation method using variable series resistance. This method implements the switch at the series and parallel resistor to generate an I-V characteristic curve similar to the PV module. The output ripple caused by switching the resistance is small since the output is regulated by the DC power supply. However, this method has a slow dynamic performance due to the large output capacitor of the DC power supply [112].

4.1.5.3. Unilluminated photovoltaic method.
The electrical circuit model of the PV model consists of a current source, diodes, and resistors, as shown in Figs. 3 and 4. The current source is linearly dependent on the irradiance and PV module temperature, as shown in (5). However, the characteristic of the diodes is too complex to represent in the equation. The unilluminated photovoltaic method is used to overcome this problem [9,24]. This method is achieved by preventing the solar irradiance from reaching the surface of the PV module. As a result, the current source represented inside the electrical circuit model of the PV module is eliminated. This current source is replaced by the external current source to allow more convenient control of the irradiance and module temperature. Therefore, there is no need to set up the artificial controllable irradiance test bed or rely on the unpredictable irradiance from the environment.

There are two ways to implement the unilluminated photovoltaic method. The first way is to use a single PV cell to generate the reference signal for the closed-loop converter system [9]. The second way is to

use the actual PV module connected to the external current source [24]. Since no controller and power converter is used for the second method, the bandwidth problem is not present when it is connected to the power conditioning system as with MPPT devices.

In conclusion, the unilluminated photovoltaic method is a simple PV emulator. The change of the irradiance is done by manipulating the external current source. The dynamic response of this method is faster since there is no complex calculation of the diode presented inside the controller. However, this method lacks flexibility since it requires the actual PV panel to operate.

4.1.5.4. Transistor based method.
The characteristic equation of a diode of the PV model is complex and burdens the digital controller. This is because the diode characteristic equation consists of the implicit equation that requires a numerical solution, such as the Newton-Raphson method, to solve the equation. The numerical solution requires multiple calculations of the same equation which leads to delays in the calculation of the operation point of the PV emulator. The complexity of the diode equation is eliminated by using the unilluminated photovoltaic method [9,24]. However, this method is not flexible since it requires the actual PV panel to act as the diode. A more convenient method is to use the network of diodes to represent the diode characteristic of the PV panel [9,49]. However, the number of diodes required is high since it depends on the number of PV cells in the PV module.

To overcome this problem, the network of diodes are replaced by the transistor [23]. The 24 cells PV module is easily represented using only three transistors. Besides the low number in the component, this method allows easier partial shading emulation since there is no processing burden, like in the digital controller, nor a high number of components, like in the diode network method. However, this method is inefficient since the transistor endures a high power loss.

4.1.6. Analysis and discussions on control strategies
Accuracy is the main concern when it comes to the PV emulator. However, the PV emulator is highly affected by the accuracy of the PV model used inside the PV emulator control system. This is because the I-V characteristic produced by the PV emulator follows the I-V characteristic of the PV model used inside the PV emulator control system if the closed-loop controlled system is implemented. However, the PV emulator accuracy is also affected by the control strategy used to determine the operating point of the PV emulator.

The direct referencing method is the commonly used control strategy for the PV emulator [7,9,10,12,25,26,34,36,48,68,87,105]. This is due to the simplicity of this method since there no additional algorithm added in the PV emulator control system. The SMPS is the commonly used power converter with the direct referencing method, as shown in Fig. 7(a) and (b) [10,18,33,40,58,95,97]. Although the SMPS is highly efficient, this type of power converter suffers from an output ripple [8,13]. The output voltage and the output current of the SMPS are constantly changing due to the turned-on and turned-off action of the power switch inside the SMPS. Since the output resistance is constant, the output ripple always moves on the inverse output resistance line, as shown in Fig. 12. Therefore, a high output ripple reduces the accuracy of the PV emulator. To overcome this problem, a larger filter is implemented on the SMPS [113]; however, this produces a slower dynamic response of the SMPS. Since the linear voltage regulator does not suffer from the output ripple problem, the output of the PV emulator is more accurate compared to the SMPS [13,82,114]. Due to the highly inefficient nature of the linear voltage regulator, the SMPS is preferable in the PV emulator application.

A PV emulator using the direct referencing method is simulated using MATLAB/Simulink® with two different output resistances. The output current of the PV emulator is shown in Fig. 13. The purpose of the simulation is to show the oscillation problem faced by the direct
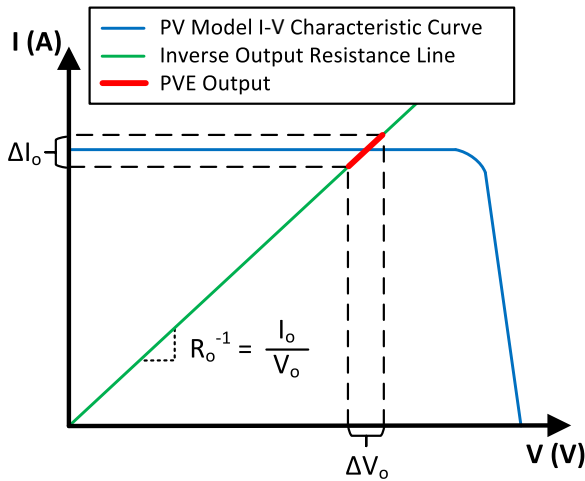
Fig. 12. The effect of output ripples on the accuracy of the PV emulator.

Fig. 14. The instability of the reference current of the PV emulator when using the direct referencing method with the closed-loop current controlled system.

referencing method at certain load conditions. The simulation started with a load resistance of 17 Ω and was reduced to 7 Ω at 0.06 s of simulation. The results show a high output current oscillation when the output resistance is 17 Ω. During this load condition, the PV emulator operates in the constant voltage region while the output current oscillation is low when the load is 7 Ω, where the PV emulator operates in the constant current region.

The output ripple produced by the SMPS causes a higher ripple of the reference signal. If the PV emulator control strategy is the direct referencing signal and the current-mode controlled is implemented, the oscillation of the reference signal is highly affected when the output resistance, R_o, is high. The higher the output resistance, the closer the operating point toward V_{oc} and zero I_{pv} on the I-V characteristic curve. The intersection between the inverse output resistance line of the high resistance and the I-V characteristic curve of the PV module is located in the constant voltage region, as shown in Fig. 14. When there is a small output voltage ripple present, it causes I_{ref} to become oscillated. As a result, I_o also oscillates. Since the change in I_o causes the change in V_o to maintain the R_o ratio, the small V_o ripple becomes larger than the original V_o ripple. This oscillation of V_o, I_{ref}, and I_o become higher until the oscillation reaches a steady state. The slower the dynamic response of the closed-loop converter system, the smaller the oscillation; there-fore, to overcome this problem, the PV emulator needs to operate as the overdamped condition.

The overdamped closed-loop converter design is a simple solution for instability problem of the direct referencing method. However, the dynamic response of the PV emulator becomes slower and takes a longer time to achieve a steady state. The PV emulator with a slow
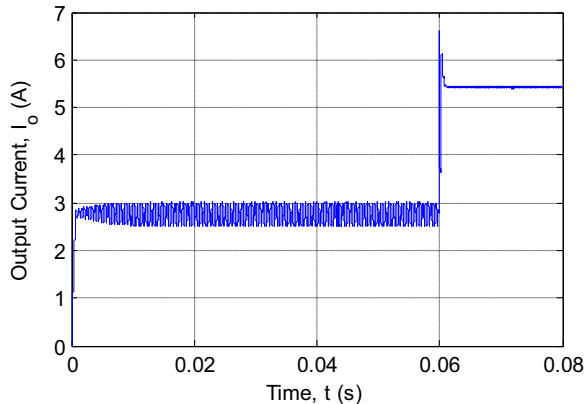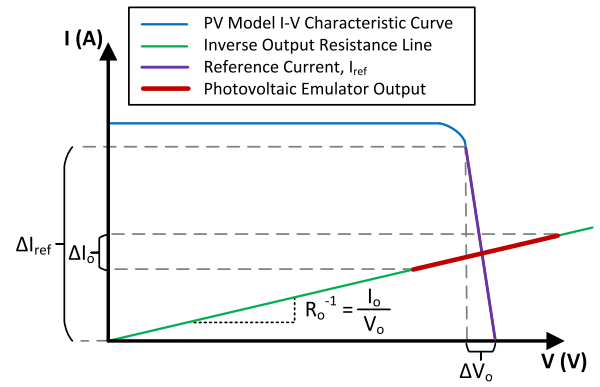

Fig. 13. The output current of the PV emulator using the direct referencing method for the output resistance of 17 Ω (0.00–0.06 s) and 7 Ω (0.06–0.08 s).

dynamic response causes problems when it is connected to the MPPT devices or the power conditioning system [46,115]. Besides the inter-face problem, a slow PV emulator does not emulate the dynamic characteristic of the actual PV module. The dynamic response of the actual PV module has approximately a few microseconds to tens of microseconds to achieve a steady state [46,115].

The dynamic response of the closed-loop buck converter system suffers a slower dynamic response when the output resistance is high. However, this effect is not observed for the PV emulator controlled using the direct referencing method. For the direct referencing method using the current-mode controlled system, I_{ref} is equal to I_{sc} during startup. Therefore, I_{ref} produced during the startup is higher than I_{ref} relative to the output resistance. As a result, the difference between I_o and I_{ref} becomes high and the high error signal is fed into the compensator of the buck converter. The high error signal causes a fast dynamic response during the PV emulator startup process. When the voltage increases, the reference current signal moves away from y-axis interception. When the reference current enters the constant voltage region, the reference current begins to drop until it reaches the reference current signal relative to the output resistance.

The hill climbing method offers a simpler control strategy com-pared to the direct referencing method. The elimination of the compensator allows the processing burden to focus on the PV model calculation instead of both the PV model and compensator. However, the constant step size of the duty cycle makes the PV emulator that uses the hill climbing method have a poor dynamic response compared to the direct referencing method.

When the output resistance is changed tremendously, the output of the PV emulator becomes unstable. During this transient period, the control strategy tries to determine the new operating point as fast as possible. The direct referencing method used the compensator that produces a dynamic duty cycle which responds faster when there is a disturbance. However, the hill climbing method used a fixed duty cycle step size. Therefore, the dynamic period takes a longer time when the output resistance is changed tremendously. The slow dynamic response is improved by increasing the duty cycle step size. However, increasing the duty cycle caused the PV emulator output to oscillate and become unstable.

The resistance comparison method is less susceptible to the output ripple. By referring to Fig. 12, the change in output voltage and output current do not affect the output resistance. When V_o increases, I_o also increases to maintain R_o ratio and vice versa. Therefore, the input signal for the PV model is more stable compared to only V_o or I_o. Thus, the reference signal produced by resistance comparison method becomes more stable.

The iteration based method is one of the resistance comparison methods. The iteration based method with the constant step size requires a high number of iterations to determine the reference point for the PV emulator [16–18]. The smaller the step size, the higher the
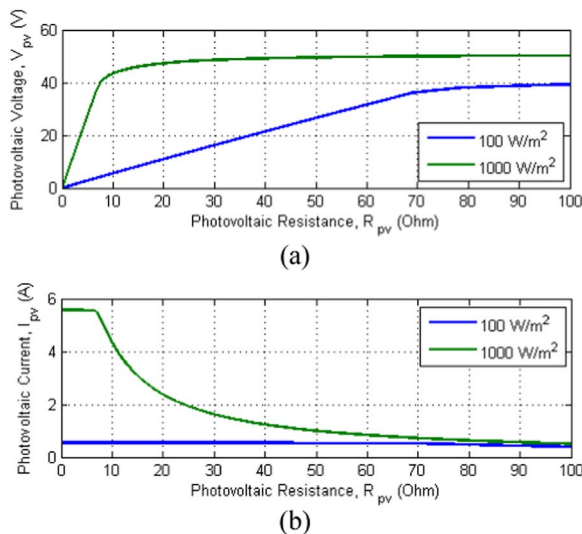
Fig. 15. a) The resistance-current and b) the resistance-voltage characteristic curve of the Sanyo HIT-215NKHE5 PV module at the module temperature of 25 ℃ with the different irradiance level [116].

number of iterations for the reference point to converge, hence, the more accurate the PV emulator output. If the step size chosen is large, the PV emulator system converges faster; however, the PV emulator output becomes inaccurate. Referring to Fig. 10, if the non-zero initial PV model input iteration based algorithm is used, a large step size produces an unconverged reference signal.

The effect of the step size of the V_{pv} and I_{pv} towards the change in R_{pv} is shown in Fig. 15(a) and (b). The analysis for the iteration based method with the voltage as the PV model input is shown in Fig. 15(a). A large step size is required if R_{pv} is below 7 Ω for the 1000 W/m^2 and below 70 Ω for 100 W/m^2, as shown in Fig. 15(a). The use of the small step size at this condition results in the slow iteration process. A small step size is required if R_{pv} is above 7 Ω for 1000 W/m^2 and above 70 Ω for 100 W/m^2. The use of a large step size at this condition results in inaccurate or unconverge results. This shows that different step sizes are required at different conditions. However, the step size used for the iteration based method of resistance comparison method is constant [16–18]. Therefore, a fast iteration process and accurate reference point are hard to achieve by using the constant step size. The analysis for the iteration based method with the current as the PV model input is shown in Fig. 15(b). The step size for this type of system requires a large step size for R_{pv} between 8 Ω and 90 Ω and the small step size for the PV resistance below 8 Ω and above 90 Ω for the irradiance of 1000 W/m^2. For the irradiance of 100 W/m^2, a larger R_{pv} is required when the I_{pv} started to reduce.

The initial value of the PV model for the iteration based method is considered when designing the PV emulator. The zero initial PV input is simpler compared to the non-zero initial output. The iteration based method continuously compared R_o with R_{pv} along the I-V characteristic curve. Even though this method is simple, the new reference signal requires time to adjust. If R_o changes, The PV emulator requires another I-V characteristic curve sweep to produce the correct reference signal depending on the condition. For the iteration based method using the PV model with the voltage as the input, if R_o decreases drastically and the PV sweeping is still lower than the new R_o, the new reference signal is produced faster. However, if the R_{pv} sweeping has passed the new R_o, the incorrect reference signal is produced momentarily before the new R_{pv} sweeping is done. Since the number of iterations is high when using a constant step size, it takes a long time to adjust the reference signal to the correct operating point.

The control strategy of the PV emulator depends on the PV model used. For the current-mode controlled system, the PV model with the

voltage as the input and the current as the output ($I = f(V)$) is required. For the voltage-mode controlled system, the PV model with the current as the input and the voltage as the output ($V = f(I)$) is required. However, the PV model with the current as the input and voltage as the output is rarely used [39,87]. The voltage-mode controlled PV emulator requires a modified PV model such as the look-up table [31,33] and piecewise linear interpolation [34,36,104]. Even though most of the PV emulator control strategies require different types of PV models for different types of closed-loop controlled modes, the resistance comparison method using the iteration based method is able to produce a voltage reference or current reference simultaneously, as shown in Table 6. The iteration based method is not affected by the type of PV model used. Therefore, this method is used for the current-mode and voltage-mode controlled system without needing a specific PV model.

4.2. Partial shading implementation

The PV cells are connected in a series to form a string which increases the voltage output. These strings are connected in parallel to increase the output current. The group of PV cells is now called the PV module. However, this type of connection suffers problem during partial shading. If one of the cells is shaded, the whole string of the PV cells produced less power and moves the maximum power point to the unexpected places [21]. The PV cell that shaded absorbed power and produced heat may damage the cell [21,60]. To overcome this problem, the bypass diode is used [60]. The purpose of the bypass diode is to protect the module from thermal damage and preserve power output if there is partial shading caused by dirt, clouds, or an object in the landscape that casts a shadow on PV cell [21]. The effect of partial shading is quantified using the field factor (FF). The FF is the ratio of maximum power over the product of the open circuit voltage and the short circuit current. The partial shading reduced the FF value [21].

The implementation of partial shading in the PV emulator is either hardware based or calculation based. The hardware based partial shading implementation does not involve any calculation to produce an I-V characteristic curve during the partial shading condition. This characteristic is generated from multiple connections of the PV emulator or multiple PV cells as the reference point. While the calculation based partial shading implementation is done using complex mathematical equations to generate the I-V characteristic curve during the partial shading condition.

4.2.1. Hardware based partial shading implementation

The hardware based partial shading implementation requires a high number of components and is costly. However, the burden of the controller is reduced since the calculation of the PV model during the partial shading condition is not included in the controller. It is implemented by connecting two programmable power supplies in a series [102]. The PV I-V characteristic is programmed in the National Instrument's LabVIEW platform. The reference point is determined using the resistance line method. The two separate I-V characteristic signals are sent to the two programmable power supplies through the serial communication support. The power-voltage (P-V) characteristic produced by the series connected programmable power supplies contains two peaks when two different reference signals are sent to the programmable power supplies. As a result, the I-V characteristic curve during the partial shading condition is produced.

Another hardware based partial shading implementation is the transistor based method [23]. Due to the low number of component used in this method, the partial shading is emulated with a lower cost compared to the programmable power supply. However, this method suffers low efficiency due to the high power loss at the transistor.

The hardware based partial shading emulation is implemented at the controller side to reduce the cost of the PV emulator. This is done

Table 6
The comparison between the different types of control strategies for the PV emulator.

Parameters	Direct referencing method	Hybrid-mode controlled method	Hill climbing method	Resistance comparison method (Iteration based method)	Resistance comparison method (Resistance line method)	Analog based control strategy
Accuracy	Accurate if stable	Accurate	Depends on the tolerance value	Depends on the tolerance value	Accurate.	Depends on the method used
Additional algorithm	Not required	Required	Required	Required	Required	Not applicable. It is based on the analog circuit
Processing burden	High processing burden	High processing burden	Lower than direct referencing method	Some of the methods have a low processing burden	–	Not applicable. It is based on the analog circuit
Software limitation	No limitation	No limitation	No limitation	No limitation	Requires line intercept detection (LabVIEW [32,45,98])	Not applicable. It is based on the analog circuit
Output stability	Unstable at a certain region of I-V characteristic curve	Stable	Unstable if the step size is large	Unstable if the step size is large	Stable	–
Convergence of the reference signal	Affected by the performance of the closed-loop converter system	Affected by the performance of the closed-loop converter system	Depends on the step size	Depends on the step size	Not applicable	–
Operating point calculation duration	Slow	Slow	Depends on the processing speed of the controller	Depends on the processing speed of the controller	–	–
Input change detection	Not applicable	Not applicable	Not applicable	Applicable	Applicable	Not applicable
Independency	Depends on the external factor	Depends on the external factor	Depends on the external factor	Independent from the external factor	Independent from the external factor	–
Step size	Variable	Variable	Constant	Constant	Constant	Not applicable
Dual reference	Not capable	Capable	Not capable	Capable	–	–

by amplifying the multiple mini PV modules using the photovoltaic amplifier method [21]. The different irradiance is generated using the light bulb controlled using analog PWM generator. The shading of the photo-diode is done by covering it with a piece of cardboard. The bypass diode is connected in parallel with the photo-diode to produce multiple peaks of the PV power-voltage (P-V) characteristic curves. This method suffers from a low efficiency problem since the PV amplifier operates in the constant voltage region.

4.2.2. Calculation based partial shading implementation

The calculation based partial shading implementation uses the mathematical equation to configure the PV cells [40,45,94,115]. For the series connection, the PV cells current are equal and the total voltage of the PV module is the sum of each PV cells voltage. For a parallel connection, the total current of the PV module is the sum of each PV cell's current, and the PV cell's voltage is equal. This method requires only a single power converter since the PV configuration is done inside the controller. The power converter is either the buck converter [40,94] or the programmable power supply [45,115].

The electrical equivalent circuit PV model consists of the implicit equation that requires an iteration process to solve. The Newton-Raphson method is commonly used to solve this implicit equation [15,45,58,71,90,98]. The calculation based partial shading implementation requires multiple numbers of PV models with different irradiances and temperatures calculated inside the controller in real-time. As a result, this complex calculation burdens the controller, reducing the sampling time. However, it is possible to directly calculate the multiple PV models for the PV emulator [15,40,94]. Several methods have been proposed to overcome this problem. One of the methods is to simplify the PV model using the characteristic curve segmentation method [40]. Another method used to reduce the processing burden is changing the equivalent circuit of the PV module into a matrix equation [115]. The PV interpolation model is also implemented to replace the complex PV electrical circuit model [45].

4.3. Hardware platform

The hardware platform for the PV emulator is implemented in the analog form, digital form or a combination of both. The PV emulator controller task is divided into two parts. The first part is to calculate the PV model and generate the reference point for the PV emulator,; the second part is to control the power converter system.

4.3.1. Analog hardware platform

The implementation of the PV model using the analog hardware platform is done to reduce the computational delay compared to the digital hardware platform [105]. The PV equivalent circuit is represented in the form of the resistance network and the series of diode stack to generate the reference signal for the closed-loop converter system [9,49]. The resistance network represents the series and parallel resistance in the PV model, while the diode stack needs to match the PV characteristic. Besides the resistance network and diode stack, the PV I-V characteristic signal is also being generated using the operational amplifier [41,46,82,105,117]. The combination of transistors and resistors are also being used in generating the I-V characteristic reference signal [23,42]. The advantage of using a transistor instead of the diode to represent the PV equivalent circuit is the reduced number of components used in the implementation process [23]. The drawback of using passive components to generate the PV characteristic is that the control of irradiance and temperature is done manually [82]. Therefore, the use of the real world data of irradiance and temperature is not applicable.

Another type of PV model using the analog hardware platform is using a single PV cell [8,9]. The operational amplifier is used to control V_{pv} of the single PV cell while I_{pv} produced by the single PV cell becomes the reference signal for the PV emulator [8]. Besides this

Table 7

The switching frequency of the power converter used in the PV emulator application using the different type of single digital hardware platform.

Digital controller type	Power converter switching frequency (kHz)			
	Analytical PV model	Look-up table	Simplified PV model	Overall
Digital Signal Processor (DSP)	6.6 [18]	13.3 [14]	33.3 [50] 50.0 [97]	6.6–50.0
dSPACE rapid prototyping	10.0 [66,92,94] 20.0 [12]	n/a	n/a	10.0–20.0
Field-Programmable Gate Array (FPGA)	30.0 [26]	50.0 [103]	46.9 [31]	30.0–50.0
Microcontroller	20.0 [17]	20.0 [39]	25.0 [76] 50.0 [37]	20.0–50.0
Computer	n/a	n/a	20.0 [10] 50.0 [84]	20.0–50.0

method, the single PV cell is used as the replacement for the diode in the electrical circuit PV model by unilluminated the PV cell [9].

The closed-loop controlled system of the power converter usually consists of the PI compensator and the pulse width modulator (PWM) [7,17,26,33,34,36,39,66,68,69,82]. However, the PI compensator and PWM are commonly implemented using the digital hardware platform since it is simpler. Even though the digital hardware platform is not susceptible to noise, it suffers from a slow calculation. A fast hardware platform is needed because the compensator is crucial, especially during the transient state of the power converter. One of the solutions is to use the operation amplifier to implement the compensator [33,46,74,82].

For the PWM, an analog hardware platform is available in the form of integrated circuit (IC) [10,16,27,33,112,118]. The switching frequency is controlled by manipulating the resistance and capacitance connected to the integrated circuit while the duty cycle signal is obtained from the compensator generated from the analog hardware platform [33] or the digital hardware platform [10,16,27]. The PWM IC allows the PV emulator to operate at a high switching frequency (up to 500 kHz) [27]; as a result, the LC filter size of the PV emulator becomes smaller and a faster dynamic response is achieved.

4.3.2. Digital hardware platform

There are two methods for implementing the digital hardware platform for the PV emulator. The PV emulator hardware platform is implemented using the single digital hardware platform or the cascade digital hardware platform. The single digital hardware platform used in the PV emulator application is the digital signal processor (DSP) [14,18,25,40,50,97,99], the dSPACE Rapid Prototyping [12,66,91,92,94], the field-programmable gate array (FPGA) [26,31,43,103], the microcontroller [13,17,27,29,37,39,76], and computer [10,48,55,58,84]. However, when the complex controller is implemented into the digital hardware platform, the digital hardware platform suffers from a large sampling time. This leads to in an incorrect control response proportional to the output of the power converter. As a result, the accuracy and stability of the PV emulator are compromised. A large sampling time also requires a low switching frequency for the SMPS. A low switching frequency increases the required filter size added, causing the dynamic response of the PV emulator to slow down.

The cascade digital hardware platform is another method used in the digital hardware platform implementation of the PV emulator. The aim of this method is to reduce the burden carried by a single digital hardware platform. The processing burden is commonly divided into two parts. The first digital hardware platform calculates the PV model for the PV emulator. The digital hardware platform used to calculate the PV model for the PV emulator is the DSP [30,119], the field-programmable analog array (FPAA) [67,68], and the microcontroller

[16,32,33,114]. The second digital hardware platform is used in controlling the closed-loop power converter system. This hardware platform is implemented with the PI compensator and the PWM. The type of hardware platform used for this task is the DSP [8], the FPAA [68], and the microcontroller [119].

The analog hardware platform is a fast system compared to the digital control. However, the analog hardware platform commonly suffers from noise problem. The implementation process for the analog hardware platform is complex. Besides, the analog hardware platform is less flexible compared to the digital hardware platform. The analog hardware platform is usually redesigned and implemented again if changes are made. The digital hardware platform is more flexible, easier to implement, and less susceptible to noise compared to the analog hardware platform.

The single digital hardware platform large sampling time problem is overcome by using a lower switching frequency of the power converter for the PV emulator system. The switching frequency of the power converter used in the PV emulator application is shown in Table 7. The maximum switching frequency handled by a single digital hardware platform is 50 kHz. However, the PV model used for a high frequency switching is either simplified or based on the data stored in the look-up table. The simplified PV model produced a lower computational time. However, the simplification results in a low accuracy [120]. For the complex analytical PV model, the switching frequency is kept low. The reduction of the switching frequency affects the output ripple, the continuous current mode operation, and the dynamic performance of the PV emulator. If the buck converter is used in the PV emulator, a large LC filter is required to maintain the continuous current mode operation and a small output voltage ripple [113]. Besides, the dynamic performance of the buck converter slows down as a result of the increase of LC filter size.

5. Power converter

The PV module is a nonlinear power supply that generates power for the load. To emulate the characteristics of the actual PV module, the PV emulator needs to generate power while having the same nonlinear characteristics as the actual PV panel. The nonlinear characteristics of the PV module are simulated using the PV model. However, the PV model only provides the signal and does not transmit power. To overcome this problem, the PV model is connected to the power converter to change the non-power transmitting PV I-V characteristic signal produced by the PV model into the power transmitting PV emulator that emulates the actual PV module I-V characteristic. There are three types of power converters used in the PV emulator application as shown in Fig. 16.

5.1. Linear regulator

The function of the linear regulator or linear dc-dc converter is to reduce the input voltage, V_i, and regulate the output. There are two ways to implement the PV emulator using the linear regulator. The first way is to implement the linear regulator using the linear regulator integrated circuit [13,82,114]. The linear voltage regulator integrated circuit (IC) is commonly chosen for the PV emulator application. However, the linear current regulator IC is also being used in the PV emulator application [13]. This type of power converter is controlled using the closed-loop PI or PID controller [13,82]. The controller is implemented in either the analog circuit using the operational amplifier or the digital circuit using the microcontroller; the servo motor can also spin the potentiometer and control of the linear regulator [114]. The linear regulator IC is capable of providing a small amount of current. Therefore, the additional current booster circuit is required to increase the rating of the PV emulator [114].

The second way to implement the linear regulator is by using the power transistor such as the bipolar junction transistor (BJT) [41,42]
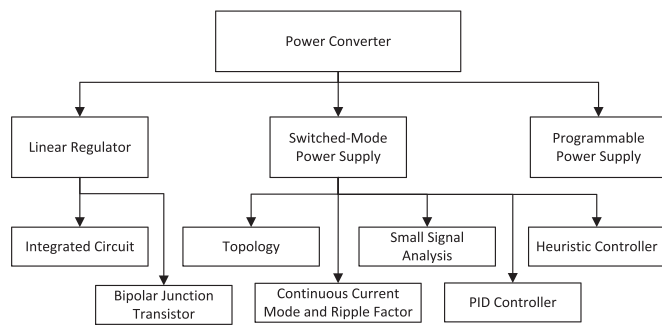
Fig. 16. The power converter used in the PV emulator application.

Fig. 17. The consideration in choosing the topology for the PV emulator.

and the MOSFET [43]. The power transistor is connected in series with the DC source and load. It performs like a variable resistor controlled by the base current (BJT) or Gate-Source Voltage, V_{gs} (MOSFET) [113]. Using the voltage divider, the change in the variable resistor represented by the power transistor allows the change in the voltage at the load. The control circuit that produces the base current for the BJT is a complex network of resistances and diodes [42] or operational amplifier [41]. The current passing through the BJT depends on a parameter called the common-emitter current gain [121]. The smaller the gain, the higher the base current is needed to control the current passing through the BJT. The base current is the control signal and it should be low. Therefore, a high common-emitter current gain is needed for a more simple control circuit design. To increase the gain, the Darlington pair is used for the current amplification [42]. The MOSFET is easier to control compared to the BJT. The control circuit that controlled V_{gs} for the MOSFET only used a voltage follower operational amplifier [43].

5.2. Switched-mode power supply

The SMPS is widely used in the PV emulator application. Since the power switch operates at the cut-off region and the saturated region, the power loss at the power switch is low which results in a highly efficient PV emulator. The SMPS output voltage is easily controlled by adjusting the duty cycle, D. The duty cycle is not connected directly to the power switch. It requires another component called the pulse width modulator (PWM) to produce pulses for the power switch according to the duty cycle.

5.2.1. Topology

There are several considerations when choosing the topology, as shown in Fig. 17. The converter with the non-galvanic isolation and the converter with the galvanic isolation are two types of SMPS used for the PV emulator. The non-galvanic isolation topology is more commonly used due to its simplicity and the low number of components required for the implementation. The buck converter is more suitable for the PV emulator since it covers a wide range of I-V characteristic curve of the PV module if the input voltage is higher than the open circuit voltage, V_{pv} [9,12,14,16–18,25,26,31,33,39,40,49,66,68,69,74,81,84,87,92,105,108]. The buck-boost and two quadrant converters are also being used in the PV emulator application with the input voltage lower than the PV I-V characteristic range [37,91]. There is also the implementation of the PV emulator using the boost converter for testing the PV grid-connected inverter system [103,122]. Another type of non-galvanic isolation topology is the Z-Source converter. However, the Z-Source converter is more difficult to control, is more costly, is less efficient, and covers less I-V characteristics at a different irradiance compared to the buck converter [28].

The galvanic isolation provides a separation between the source and the load. This is done by implementing the transformer into the topology. This type of topology is also suitable for the PV emulator if the voltage difference between the input voltage and the output voltage is too large. This is done by manipulating the turn ratio of the primary
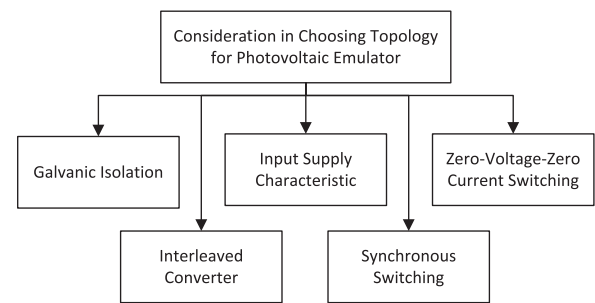
and secondary winding. The step-down converter used in the PV emulator application is the forward converter [58,97]. There is also the step-up and step-down converter for the PV emulator application which is the flyback converter [32,76,119]. Since the transformer is involved in this topology, the transformer design is considered. Although the number of the components required for the flyback converter is low, this converter requires a large transformer core as the power requirement increases [113,123]. This topology is suitable for emulating the PV module up to 150 W [113]. The forward transformer is more suitable for the PV emulator application since it able to operate up to 500 W [113]. However, this converter requires an extra filter inductor which increases the PV emulator cost. A disadvantage of using the flyback converter and the forward converter is that the power switch must withstand the high voltage stress when the switch is off.

There is also the use of interleaved buck converter in the PV emulator application [8]. The interleaved buck converter or multiphase buck converter has more advantages compared to the conventional buck converter. The noticeable different between these two DC-DC converters are the interleaved buck converter has lower inductor current ripple compared to the conventional buck converter [113,124,125]. As a result, the lower capacitance requires the interleaved buck converter to maintain the same ripple factor as the conventional buck converter. The low capacitance improves the dynamic performance of the converter [124–128]. This allows the interleaved buck converter to have a higher bandwidth and faster response compared to the conventional buck converter with the same output resistance range and switching frequency. In addition to the dynamic performance, the efficiency of the interleaved buck converter is also higher compared to the conventional buck converter [124–126,129]. The non-ideal MOSFET and the inductor have an internal series resistor and an increase in the current passing through these components increases the power loss exponentially which reduces the efficiency of the converter, as shown in Eq. (8). The current passing through the diodes, MOSFETs, and inductors are divided into each stage of the interleaved buck converter. Therefore, the efficiency of the interleaved buck converter is higher compared to the conventional buck converter. The smaller rating of the MOSFET uses an interleaved buck converter compared to the conventional buck converter results in a lower internal series resistance. According to Eq. (8), decreases in the internal series resistance results in decreases of power loss and improves the power converter efficiency. The interleaved buck converter is able to operate at a much lower duty cycle [129,130]. Therefore, the interleaved is able to operate at a higher input voltage and a wider PV I-V characteristic emulation. The voltage stress endured by the MOSFET in the interleaved buck converter is also reduced compared to the conventional buck converter [131]. The disadvantages of the interleaved buck converter are the complex controller, a high number of components, and high sensitivity toward the unsymmetrical duty cycle [126,130,132,133]. The unsymmetrical duty cycle between the stages causes an unbalanced division of current passing through the inductor [130,132,133]. As a result, a higher current passes through the inductors, MOSFETs and the diodes than the rated current which damages the converter.

$$P_{loss} = I_{pass}^2 R_{int(ser)} \qquad (8)$$

where P_{loss} is the power loss (W), I_{pass} is the current passing through the component (A), and $R_{int(ser)}$ is the internal series resistance of the component (Ω).

The input supply characteristic is considered when choosing the power converter for the PV emulator. The PV emulator with the ability to emulate multiple PV modules requires higher input power. This input power is commonly obtained from a three phase supply [34,134]. For the single module to the double module emulation, a single phase power supply is sufficient. The PV emulator commonly uses the DC power supply as the input supply. However, the unregulated rectifier is also being used before the rectified output is connected to the DC-DC converter [14,16,34,40,74,76,84,97]. There is also the use of the regulated rectifier to reduce the input voltage for the DC-DC converter [8] or directly emulate the PV I-V characteristic [7,134]. The use of the regulated rectifier in only the PV emulator application reduced the number of converters needed for the PV emulator with AC input.

The synchronous buck converter is also used in the PV emulator application [20,29,46,99]. This type of converter used the synchronous switching or synchronous rectification to improve the efficiency of the converter [29,99,113,135]. The power loss of the diode inside the conventional buck converter topology is caused by the forward voltage drop. By adding the MOSFET (synchronous rectifier) parallel to the diode, the voltage drop is reduced which results in a lower power loss. The topology becomes the synchronous buck converter when the synchronous rectifier is added into the conventional buck converter circuit. The control circuit of the synchronous buck converter is more complex compared to the conventional buck converter since the two MOSFETs are controlled. Moreover, the time delay between switching (dead time) is required to prevent a short circuit. The diode is not removed in the synchronous buck converter to allow the inductor current to flow during the dead time. Even though there is already a parallel diode implemented inside the MOSFET, this diode has a slow reverse recovery characteristic and it reduces the efficiency of the converter. The synchronous buck converter is further improved by implementing the transformer driver or the voltage mirror driver [135].

The zero-voltage-zero-current (ZVZC) switching or soft switching is also considered in the PV emulator [36,95]. This switching technique reduces the power loss and improves the efficiency of the converter [135,136]. The conventional converter uses the switching technique called hard switching that causes a large change in the voltage and current. As a result, the switching loss increases, and an electromagnetic interference (EMI) is produced. The switching loss and the EMI are reduced by implementing the soft switching, which is categorized into zero-voltage switching (ZVS) and zero-current switching (ZCS). However, the soft switching requires variable switching frequency, increases the device stresses, and causes conduction loss [135].

5.2.2. Continuous current mode and ripple factor

The continuous current mode and the ripple factor are the two considerations in designing the SMPS for the PV emulator. The PV emulator is recommended by the researcher to operate in the continuous current mode, while the ripple factor is kept below 2% [34,66,108]. The PV emulator is implemented using various types of topology. However, the buck converter is commonly used for the PV emulator application due to the low number of components and the simple design. Therefore, the analysis of the continuous current mode and the ripple factor is focused on in the buck converter.

The continuous current mode depends on the output resistance and the switching frequency. A large inductance is needed for a high output resistance, and a small inductance is required for a high switching frequency. The minimum inductance to maintain the continuous current mode, L_{min}, for the buck converter is shown in Eq. (9) [113].

$$L_{min} = \frac{(1 - D)R}{2f} \qquad (9)$$

where D is the duty cycle, R is the output resistance (Ω), and f is the switching frequency (Hz).

The output voltage ripple factor is also considered for the PV emulator. A good PV emulator should have a low ripple factor. However, the smaller ripple factor requires a larger capacitance. The larger capacitance causes the buck converter to have the poor dynamic response.

$$C = \frac{1 - D}{8Lr_v f^2} \qquad (10)$$

where L is the inductance used in the buck converter (H), r_v is the output voltage ripple factor ($\Delta V_o/V_o$), ΔV_o is the output voltage ripple (V), and V_o is the output voltage (V).

5.2.3. Small signal analysis

The small signal analysis is used in designing the closed-loop control system. The function of the small signal analysis is to produce a transfer function that represents the power converter. By using this transfer function, the design of the controller is done precisely instead of relying on the trial−and-error method.

There are many ways to perform the small signal analysis of the power converter, including the current injecting approach, circuit averaging, averaged switch modeling, behavioral modeling and the state space averaging method [29,81,136,137]. The converter transfer properties for every method used are the same. However, there are advantages and disadvantages to each method used. The current injection method is a simple small signal analysis method and it is suitable for the discontinuous current mode operation [138]. The state space averaging method is used for a complicated converter structure modeling [138]. However, the state space averaging method for the discontinuous current mode is very complex. Since the PV emulator needs to operate in the continuous current region, the state space averaging method is used in the small signal analysis.

The state space averaging method is commonly used in the PV emulator application. The analysis is started by analyzing the state of the circuit during the closed switch and the open switch condition. The analysis focuses on the energy storage components such as the inductor and capacitor. The SMPS DC-DC converter usually depends on the duty cycle. Therefore, the analysis of the different state of the converter is averaged according to the duty cycle. The averaged equation is then rearranged according to the state space as shown in Eq. (11), while the output equation is arranged as shown in Eq. (12). Eqs. (11) and (12) are known as the state space representation. However, the transfer function is more convenient in a controller design compared to the state space representation. Therefore, the state space representation is converted into the transfer function by using Eq. (13).

$$\dot{x} = Ax + Bu \qquad (11)$$

$$y = Cx + Eu \qquad (12)$$

$$G(s) = \frac{\hat{y}(s)}{\hat{u}(s)} = C(sI - A)^{-1}B + D \qquad (13)$$

where $\dot{x}$ is the first order of the state space vector, x is state space vector, u is input vector, y is output vector, A is the system matric, B is the input matric, C is the output matric, E is the feedforward matric, I is the identity matric, G is the transfer function, $\hat{y}$ is the small signal term of the output, and $\hat{u}$ is the small signal term of the input.

Since the buck converter is commonly used in the PV emulator application, the converter transfer function obtained from the small signal analysis is shown in Eqs. (14) and (15) [9,17,33,66,68, 108,113,139−143]. The non-ideality of the buck converter is also considered in the small signal analysis to obtain a more precise transfer function [12,25,39,81,105,140,144,145]. The non-ideality considered

in the buck converter is the inductor internal series resistance, r_L, and the equivalent series resistance (ESR) of the capacitor, r_C. However, the effect of the r_L and r_C are insignificant since the values are very small. The transfer function of the other SMPS used in the PV emulator such as the interleaved buck converter [8], the synchronous buck converter [46], the boost converter [103,122], and the flyback converter [32,76,119] is also presented.

$$G_{v(bc)}(s) = \frac{\hat{v}_o(s)}{\hat{d}(s)} = V_i \frac{1/LC}{s^2 + 1/RCs + 1/LC} \tag{14}$$

$$G_{i(bc)}(s) = \frac{\hat{i}_o(s)}{\hat{d}(s)} = \frac{V_i}{R} \frac{1/LC}{s^2 + 1/RCs + 1/LC} \tag{15}$$

where $G_{v(bc)}(s)$ and $G_{i(bc)}(s)$ are the transfer functions of the buck converter, $\hat{v}_o(s)$ is the small signal of the output voltage, $\hat{i}_o(s)$ is the small signal of the output current, and $\hat{d}(s)$ is the small signal of the duty cycle.

5.2.4. PID controller

The PI controller [7,17,21,26,33,34,36,39,66,68,69,82] and the PID controller [9,12,13,25,46,49,97,119] are widely used in the PV emulator application. By referring to Eq. (16), the PID controller consists of the proportional gain (K_p), integral gain (K_i), and derivative gain (K_d). By manipulating these gains, the dynamic performance of the power converter improves. The PI controller is the PID controller with zero K_d. The cascade PI controller is also implemented in the PV emulator application to improve the dynamic performance and prevent the converter from being damaged [34].

The PID controllers are either implemented as the voltage-mode controlled system, as shown in Fig. 18(a) [25,26,34,66,68,69,81,97] or as the current-mode controlled system, as shown in Fig. 18(b) [9,10,17,24,33,35,50,82,103,122]. Since the reference signal, Ref, is not constant due to the nonlinear characteristic of the PV module, there is also the hybrid-mode controlled system that combines the voltage-mode and current-mode controlled system to improve the performance of the PV emulator [13,14]. By referring to Fig. 18(a) and (b), the design of the PID controller requires the transfer function of the converter used. Therefore, a small signal analysis is performed on the power converter before proceeding to the design of the PID controller. However, the small signal analysis is a complicated process and leads to the absence of the transfer function. As a result, the PID controller is designed using the trial-and-error method.

$$G_c(s) = K_p + \frac{K_i}{s} + K_d s = \frac{K_d s^2 + K_p s + K_i}{s} \tag{16}$$

There are several ways to design the PID controller in the PV emulator application. The PID controller in the PV emulator application is designed using the empirical method [97], the k-factor method [76,119], the z-transform method [36], the pole placement method [10,12,25,74,81,94], the lead/lag compensator [33], or the system margin adjustment [9,17,33,39,49,103,122]. The system margin ad-
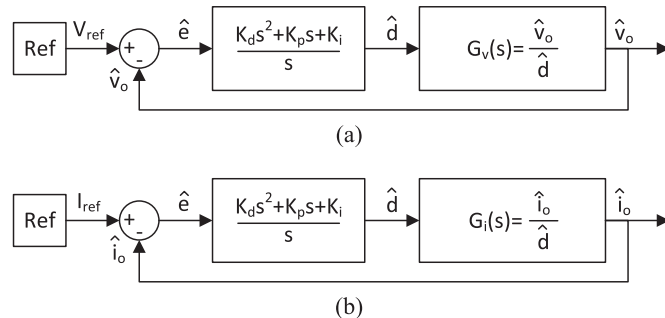
justment is widely used in the PV emulator application since the method is easy to implement. The stability analysis of the closed-loop system is done using the open-loop system [146]. The output of the closed-loop system becomes infinity as the output of the open-loop system reach -1 or 0 dB 180º. To ensure the closed-loop system is stable, the open-loop system has to be further than -1 point. The distance of the open-loop system output from the -1 point the system margin. The further the system from the -1 point, the more stable the system. This is done by tuning the gains in the PID controller.

5.2.5. Advance controller

The PI controller is the commonly used controller in the PV emulator application and the controller usually uses fixed gain values. However, the load of the PV emulator is varied and different gains of PID controller are needed for the optimum dynamic performance. The fuzzy PI controller is implemented to produce an adaptable PI controller according to the load of the PV emulator [10]. It is based on the Takagi-Sugeno fuzzy model that allows the controller to adaptively regulate the gains of the PI controller according to the change of operation point.

Besides the fuzzy PI controller, the sliding mode control is also being used in the PV emulator application [29,91]. The advantage of the sliding mode control is its fast response and the robustness of the controller. However, this type of controller is restricted by the switching frequency of the power switch. Due to this restriction, the power switch is controlled by the hysteresis comparator to ensure the sliding surface is close to zero.

The double current mode controlled is also being used in the PV emulator application [29]. This control method is called the predictive current control. The outer current loop uses the PID controller that compares the reference current and the output current. This PID controller produces the appropriate average inductor current. While the inner current loop controls the duty cycle depending on the average inductor current. Even though this control method is complex, it is immune to high noises and is more stable [29].

5.3. Programmable power supply

The PV emulator implementation using the programmable power is simpler compared to other power converters [15,44,70,72,73,98,102]. This implementation method does not require the converter controller since the programmable power supply already includes the converter controller. The only component required is the PV model which produces the PV I-V characteristic signal required by the programmable power supply. The PV model is implemented using LabVIEW software. LabVIEW is a high-level graphic programming language which has fast executing capabilities compared to other programming languages [72]. The LabVIEW also provides a 284 PV panel characteristic database called Sandia PV Database that is used to test the accuracy of the PV model [70]. The signal produced by the LabVIEW program in the computer is sent to the programmable power supply using communication interface. The programmable power supply such as the Philips-Fluke PM2832 requires an additional communication interface such as the National Instrument GPIB Controller to operate [72]. There is also the programmable power supply like the TDK-Lambda that has a built-in communication interface [102]. Besides LabVIEW, MATLAB/Simulink is also used with the programmable power supply. The dSPACE 1104 is used as the communication interface between the computer and XR Series Magna programmable power supply and the graphical user interface (GUI) is built using the dSPACE Control Desk software provided by dSPACE [73].

The disadvantage of the PV emulator using the programmable power supply is the response delay. The time taken for the programmable power supply output voltage and current to respond to the load, irradiance, and temperature change are quite long compared to other power converter. A PV emulator using the programmable power supply

(a)

(b)

Fig. 18. The closed-loop controlled system using the PID controller for a) the voltage-mode controlled system and b) the current-mode controlled system.

Table 8
The comparison between the power converters used in the PV emulator application.

Parameters	Linear voltage regulator	Switching-mode power supply	Programmable power supply
Efficiency	Very low efficiency	High efficiency	n/a
Output ripple	No output ripple	Has a ripple. Affects the accuracy and the stability of the PV emulator	n/a
Dynamic performance	n/a	Fast dynamic performance	Very slow dynamic performance
Electrical isolation	No electrical isolation	Depends on the topology	n/a
Converter controller	Required	Required	There is no need to design the controller

takes 120 ms to respond when the new voltage level is set at the programmable power supply [102]. A PV emulator using the programmable power supply and implemented using LabVIEW takes around 400 ms to process the entire loop of the algorithm, which includes the 233 ms to set up the programmable power supply [70]. Another programmable power supply based PV emulator using the analog control implementation has a response time of 3.8 ms [49], while the transient response time for the programmable power supply based PV emulator using dSPACE 1104 control system takes 0.015 ms when a sudden change in irradiance occurs [66].

5.4. Discussions on power converters

In the PV emulator application, the linear regulator is rarely used since the efficiency of this power converter is low [113]. The linear regulator efficiency depends on the reduction of the input voltage. The linear regulator is generally connected in series with the power supply and the load. Therefore, the current flowing through the linear regulator, power supply, and load is approximately the same. Since the system is in series, the voltage across the linear regulator and the load is equal to the voltage across the power source; the lower the output voltage, the higher the voltage across the linear regulator. However, the switch inside the SMPS operates at completely off or completely on conditions. As a result, the power loss is reduced and the efficiency of the SMPS is almost 90%. By referring to Table 8, the SMPS is more suitable for the PV emulator application compared to the linear regulator in terms of efficiency.

The linear regulator has no output ripple [13]. Since the PV module has no voltage and current ripple, the PV module is emulated more accurately when using this topology. However, the SMPS contains the output ripple due to the switching action. As a result, the PV module characteristic is not emulated accurately. Besides the accuracy, the stability of the PV emulator is also compromised due to the output ripple. If the direct referencing method is used, the output ripple causes the reference point for the PV emulator to become oscillated. Oscillation of the reference point further increases the output ripple. Therefore, the linear regulator is better than the SMPS in terms of accuracy and stability due to the lack of output ripple as shown in Table 8.

The dynamic performance of the SMPS is better than the programmable power supply. The PV module dynamic performance depends on the PV voltage. The actual PV module dynamic response duration is around a 10th of microsecond [46]. However, the performance of the PV emulator using the SMPS and the programmable power supply is around a 10,000th and 100,000th of microsecond, respectively. The PV emulator must have a higher bandwidth characteristic compared to the MPPT devices to allow the system to work properly. Therefore, the SMPS is more suitable for the PV emulator application compared to the programmable power supply in terms of dynamic performance, as shown in Table 8.

The SMPS topologies, such as the flyback converter and the forward converter, have an electrical isolation that is able to separate the ground between input and the output. This is done by introducing the transformer into the circuit. However, the linear regulator does not have electrical isolation. Therefore, in terms of safety, the SMPS with

electrical isolation is better than the linear regulator.

The linear regulator and the SMPS require controller design such as PID controller to allow the power converter to operate as the PV emulator. However, the design process of the converter controller is very complex. The transfer function of the power converter is required for the systematic design of the PID controller. To obtain the transfer function, a complex small signal analysis is done which requires a strong knowledge of mathematic analysis and circuit theory. However, the converter controller is already integrated inside the programmable power supply. Therefore, the design of the PV emulator using the programmable power supply is simpler compared to the linear regulator and the SMPS.

6. Conclusion

This paper has been organized and structured so that the researcher develops a basic idea of the PV emulator, ranging from the PV model, the control strategy, and the power converter. The review on the PV emulator assists the researcher on the information gathering process, which saves a lot of time. The design criteria of the PV emulator depend on the accuracy of the output, the efficiency of the system, and the ability of the system to determine the operating point at a fast rate. Based on the literature review, it can be concluded that the direct referencing method, the hill climbing method, or the perturb and observe method are simple to implement. However, these control strategies have a poor dynamic performance and oscillating output. This issue is overcome by using the hybrid-mode controlled method or the resistance comparison method, which produces a more stable operating point for the PV emulator. Nevertheless, these control strategies have a complex design. The processing burden to calculate the PV model is also challenge in designing the PV emulator. A lot of research has been done to reduce the processing burden by modifying the PV model or using the analog based method. The efficiency of the PV emulator is affected by the power converter. The SMPS has a high efficiency but produces an output ripple, while the linear regulator has a low efficiency but no output ripple. Both SMPS and linear regulator required a closed-loop controlled system design. However, the programmable power supply does not require the closed-loop controlled system, but has a slow transient response. The PV emulator is a useful device for the researcher and the industrial sector to study the solar energy generation system. Therefore, it is hoped that this review can further improve the performance of the PV emulator.

References

[1] REN21. Renewables 2016 Global Status Report (GSR); 2016.
[2] Belhamadia A, Mansor M, Younis MA. Assessment of wind and solar energy potentials in Malaysia. In: IEEE conference on clean energy and technology (CEAT); 2013, p. 152–157.
[3] E. Commission. Malaysia Energy Information Hub (MEIH). Available: ⟨http://meih.st.gov.my/statistics⟩.
[4] Armstrong S, Lee CK, Hurley WG. Investigation of the harmonic response of a photovoltaic system with a solar emulator. In: European conference on power electronics and applications , ; 2005, p. 8.
[5] Ametek Programmable Power. Available: ⟨http://www.programmablepower.com/⟩.
[6] Magma Power. Available: ⟨http://www.magna-power.com/⟩.
[7] Roncero-Clemente C, Romero-Cadaval E, Minambres V, Guerrero-Martinez M, Gallardo-Lozano J. PV array emulator for testing commercial PV inverters.

Elektron Ir Elektro 2013;19:71–5.

[8] Koran A, LaBella T, Lai JS. High efficiency photovoltaic source simulator with fast response time for solar power conditioning systems evaluation. IEEE Trans Power Electron 2014;29:1285–97.

[9] Koran A, Sano K, Rae-Young K, Jih-Sheng L. Design of a photovoltaic simulator with a novel reference signal generator and two-stage LC output filter. IEEE Trans Power Electron 2010;25:1331–8.

[10] Zhang J, Wang S, Wang Z, Tian L. Design and realization of a digital PV simulator with a push-pull forward circuit. J Power Electron 2014;14:444–57.

[11] Abbes D, Martinez A, Champenois G, Robyns B. Real time supervision for a hybrid renewable power system emulator. Simul Model Pract Theory 2014;42:53–72, [3//].

[12] Di Piazza MC, Pucci M, Ragusa A, Vitale G. Analytical versus neural real-time simulation of a photovoltaic generator based on a DC-DC converter. IEEE Trans Ind Appl 2010;46:2501–10.

[13] Kim Y, Lee W, Pedram M, Chang N. Dual-mode power regulator for photovoltaic module emulation. Appl Energy 2013;101:730–9.

[14] Yuan L, Taewon L, Peng FZ, Dichen L. A hybrid control strategy for photovoltaic simulator. In: Twenty-fourth annual IEEE in applied power electronics conference and exposition, 2009. APEC; 2009, p. 899–03.

[15] Mai TD, De Breucker S, Baert K, Driesen J. Reconfigurable emulator for photovoltaic modules under static partial shading conditions. Sol Energy 2017;141:256–65, [1/1/].

[16] Qingrong Z, Pinggang S, Liuchen C. A photovoltaic simulator based on DC chopper. In: Canadian conference on electrical and computer engineering, 2002. IEEE CCECE. Vol. 1; 2002, p. 257–61.

[17] Balakishan CH, Sandeep N. Development of a microcontroller based PV emulator with current controlled DC-DC buck converter. Int J Renew Energy Res 2014;4:1, [22/11/14].

[18] Rana AV, Patel HH. Current controlled buck converter based photovoltaic emulator. J Ind Intell Inf 2013;1.

[19] Erkaya Y, Moses P, Flory I, Marsillac S, Ieee. Development of a solar photovoltaic module emulator. In: Proceedings of the 42nd photovoltaic specialist conference, New York; 2015.

[20] Gonzalez-Llorente J, Rambal-Vecino A, Garcia-Rodriguez LA, Balda JC, Ortiz-Rivera EI. Simple and efficient low power photovoltaic emulator for evaluation of power conditioning systems. In: 2016 IEEE applied power electronics conference and exposition (APEC); 2016, p. 3712–6.

[21] Midtgard OM. A simple photovoltaic simulator for testing of power electronics. In: 2007 European conference on power electronics and applications; 2007, p. 1–10.

[22] Nagayoshi H. I–V curve simulation by multi-module simulator using I–V magnifier circuit. Sol Energy Mater Sol Cells 2004;82:159–67, [5/1/].

[23] Zegaoui A, Aillerie M, Petit P, Charles J-P. Universal transistor-based hardware simulator for real time simulation of photovoltaic generators. Sol Energy 2016;134:193–201, [9//].

[24] Zhou Z, Holland PM, Igic P. MPPT algorithm test on a photovoltaic emulating system constructed by a DC power supply and an indoor solar panel. Energy Convers Manag 2014;85:460–9, [9//].

[25] Di Piazza MC, Pucci M, Ragusa A, Vitale G. A grid-connected system based on a real time PV emulator: Design and experimental set-up. In: IECON 2010 Proceedings of the 36th annual conference on IEEE industrial electronics society; 2010, p. 3237–43.

[26] Ickilli D, Can H, Parlak KS. Development of a FPGA-based photovoltaic panel emulator based on a DC/DC converter. In: 2012 38th IEEE photovoltaic specialists conference (PVSC); 2012, p. 001417–21.

[27] Erkaya Y, Moses P, Flory I, Marsillac S. Steady-state performance optimization of a 500 kHz photovoltaic module emulator. In: 2016 IEEE Proceedings of the 43rd photovoltaic specialists conference (PVSC); 2016, p. 3205–8.

[28] Iqbal MT, Tariq M, Ahmad MK, Arif MSB. Modeling, analysis and control of buck converter and Z-source converter for photo voltaic emulator. In: 2016 IEEE Proceedings of the 1st international conference on power electronics, intelligent control and energy systems (ICPEICES); 2016. p. 1–6.

[29] Weichao Z, Kimball JW. DC-DC converter based photovoltaic simulator with a double current mode controller. In: 2016 IEEE power and energy conference at Illinois (PECI); 2016, p. 1–6.

[30] Gadelovits S, Sitbon M, Kuperman A. Rapid prototyping of a low-cost solar array simulator using an off-the-shelf DC power supply. IEEE Trans Power Electron 2014;29:5278–84.

[31] Koutroulis E, Kalaitzakis K, Tzitzilonis V. Development of an FPGA-based system for real-time simulation of photovoltaic modules. Microelectron J 2009;40:1094–102.

[32] Barrera LM, Osorio RA, Trujillo CL. Design and implementation of electronic equipment that emulates photovoltaic panels. In: 2015 IEEE 42nd photovoltaic specialist conference (PVSC); 2015, p. 1–5.

[33] González-Medina , Patrao Raúl, Garcerá Iván, Figueres Gabriel, Emilio . A low-cost photovoltaic emulator for static and dynamic evaluation of photovoltaic power converters and facilities. Prog Photovolt: Res Appl 2012;22:227–41.

[34] Martin-Segura G, Lopez-Mestre J, Teixido-Casas M, Sudria-Andreu A. Development of a photovoltaic array emulator system based on a full-bridge structure. In: Proceedings of the 9th international conference on electrical power quality and utilisation, 2007. EPQU 2007; 2007, p. 1–6.

[35] Abidi H, Ben Abdelghani AB, Montesinos-Miracle D. MPPT algorithm and photovoltaic array emulator using DC/DC converters. In: 2012 16th IEEE mediterranean electrotechnical conference (MELECON); 2012, p. 567–72.

[36] Ziming Z, Jianwen Z, Haimeng S, Gang W, Xiwen H, Shi Z. Research on photovolta array emulator system based on a novel zero-voltage zero-current switching converterer. In: Power and energy engineering conference (APPEEC), 2010 Asia-Pacific; 2010, p. 1–4.

[37] Lu DDC, Nguyen QN. A photovoltaic panel emulator using a buck-boost DC/DC converter and a low cost micro-controller. Sol Energy 2012;86:1477–84, [5//].

[38] Gomez-Castaneda F, Tornez-Xavier GM, Flores-Nava LM, Arellano-Cardenas O, Moreno-Cadenas JA, Ieee. Photovoltaic panel emulator in FPGA technology using ANFIS approach. In: Proceedings of the 11th international conference on electrical engineering, computing science and automatic control (Cce); 2014, p. 6.

[39] Vijayakumari A, Devarajan AT, Devarajan N. Design and development of a model-based hardware simulator for photovoltaic array. Int J Electr Power Energy Syst 2012;43:40–6, [12//].

[40] Chen C-C, Chang H-C, Kuo C-C, Lin C-C. Programmable energy source emulator for photovoltaic panels considering partial shadow effect. Energy 2013;54:174–83, [6/1/].

[41] Schofield DMK, Foster MP, Stone DA. Low-cost solar emulator for evaluation of maximum power point tracking methods. Electron Lett 2011;47:208–9.

[42] Tang K-H, Chao K-H, Chao Y-W, Chen J-P. Design and implementation of a simulator for photovoltaic modules. Int J Photo 2012;2012.

[43] Jin S, Zhang D. A simple control method of open-circuit voltage for the FPGA-based solar array simulator. In: IEEE international conference on power and renewable energy (ICPRE); 2016, p. 209–216.

[44] Rajguru V, Gadge K, Karyakarte S, Kawathekar S, Menon V. Design and implementation of a prototype DC photovoltaic power system simulator with Maximum Power Point Tracking system. In: 2016 IEEE Proceedings of the 1st international conference on power electronics, intelligent control and energy systems (ICPEICES); 2016, p. 1–5.

[45] Xenophontos A, Rarey J, Trombetta A, Bazzi AM. A flexible low-cost photovoltaic solar panel emulation platform. In: Proceedings of the power and energy conference at Illinois (PECI); 2014, p. 1–6.

[46] Nguyen-Duy K, Knott A, Andersen MAE. High dynamic performance nonlinear source emulator. IEEE Trans Power Electron 2016;31:2562–74.

[47] Piazza MCD, Vitale G. Photovoltaic sources: modelling and emulation. Springer Science & Business Media; 2012.

[48] Agrawal J, Aware M. Photovoltaic system emulator. In: 2012 IEEE international conference on power electronics, drives and energy systems (PEDES); 2012, p. 1–6.

[49] Koran AM. Photovoltaic source simulators for solar power conditioning systems: design optimization, modeling, and control. Blacksburg, Virginia: Doctor of Philosophy Virginia Polytechnic Institute and State University; 2013.

[50] Lee J-P, Min B-D, Kim T-J, Kim J-H, Ryu M-H, Baek J-W. et al., Development of a photovoltaic simulator with novel simulation method of photovoltaic characteristics. In: 31st international telecommunications energy conference, 2009. INTELEC; 2009, p. 1–5.

[51] Cubas J, Pindado S, Victoria M. On the analytical approach for modeling photovoltaic systems behavior. J Power Sources 2014;247:467–74.

[52] De Blas M, Torres J, Prieto E, Garcıa A. Selecting a suitable model for characterizing photovoltaic devices. Renew Energy 2002;25:371–80.

[53] Hyeonah P, Hyosung K. PV cell modeling on single-diode equivalent circuit. In: Proceedings of the 39th annual conference of the IEEE industrial electronics society, IECON; 2013, p. 1845–9.

[54] Lingyun X, Lefei S, Wei H, Cong J. Solar cells parameter extraction using a hybrid genetic algorithm. In: Proceedings of the third international conference on measuring technology and mechatronics automation (ICMTMA); 2011, p. 306–9.

[55] Agrawal JH, Aware MV. Photovoltaic simulator developed in LabVIEW for evalution of MPPT techniques. In: 2016 International conference on electrical, electronics, and optimization techniques (ICEEOT); 2016, p. 1142–7.

[56] De Soto W, Klein S, Beckman W. Improvement and validation of a model for photovoltaic array performance. Solar energy, 80; 2006, p. 78–88.

[57] Ishaque K, Salam Z, Syafaruddin . A comprehensive MATLAB Simulink PV system simulator with partial shading capability based on two-diode model. Sol Energy 2011;85:2217–27, [9//].

[58] Atoche AC, Castillo JV, Ortegón-Aguilar J, Carrasco-Alvarez R, Gío JS, Colli-Menchi A. A high-accuracy photovoltaic emulator system using arm processors. Sol Energy 2015;120:389–98.

[59] Attivissimo F, Nisio AD, Savino M, Spadavecchia M. Uncertainty analysis in photovoltaic cell parameter estimation. Instrum Meas IEEE Trans 2012;61:1334–42.

[60] Belhaouas N, Cheikh MA, Malek A, Larbes C. Matlab-Simulink of photovoltaic system based on a two-diode model simulator with shaded solar cells. Rev RER 2013;16:65–73.

[61] Chowdhury S, Chowdhury S, Taylor G, Song Y. Mathematical modelling and performance evaluation of a stand-alone polycrystalline PV plant with MPPT facility. In: Power and energy society general meeting-conversion and delivery of electrical energy in the 21st Century, 2008 IEEE; 2008, p. 1–7.

[62] Di Piazza MC, Luna M, Ragusa A, Vitale G. A dynamic model of a photovoltaic generator based on experimental data. Renew Energy Power Qual J ISSN 2010.

[63] Gow J, Manning C. Development of a photovoltaic array model for use in power-electronics simulation studies. Electr Power Appl IEE Proc 1999:193–200.

[64] Jervase JA, Bourdoucen H, Al-Lawati A. Solar cell parameter extraction using genetic algorithms. Meas Sci Technol 2001;12:1922.

[65] Sandrolini L, Artioli M, Reggiani U. Numerical method for the extraction of photovoltaic module double-diode model parameters through cluster analysis. Appl Energy 2010;87:442–51.

[66] Azharuddin SM, Vysakh M, Thakur HV, Nishant B, Babu TS, Muralidhar K, et al. A near accurate solar PV emulator using dSPACE controller for real-time control. Energy Procedia 2014:2640–8.

[67] Balato M, Costanzo L, Gallo D, Landi C, Luiso M, Vitelli M. Design and implementation of a dynamic FPAA based photovoltaic emulator. Sol Energy 2016;123:102–15, [1//].

[68] Barra F, Balato M, Costanzo L, Gallo D, Landi C, Luiso M, et al., Dynamic and reconfigurable photovoltaic emulator based on FPAA; 2014.

[69] Dolan D, Durago J, Crowfoot J, Taufik, Simulation of a photovoltaic emulator. In: North American power symposium (NAPS), 2010; 2010, p. 1–7.

[70] Durago JG. Photovoltaic emulator adaptable to irradiance, temperature and panel-specific I–V curves. California, United States: Master of Science in Electrical Engineering, Electrical Engineering, California Polytechnic State University, San Luis Obispo; 2011.

[71] Lee W, Kim Y, Wang Y, Chang N, Pedram M, Han S. Versatile high-fidelity photovoltaic module emulation system. In: Proceedings of the 17th IEEE/ACM international symposium on low-power electronics and design; 2011. p. 91–6.

[72] Bernal PG. Study and development of a photovoltaic panel simulator. Faculdade de Engenharia da Universidade do Porto: Master in Electrical and Computers Engineering University of Porto; 2012.

[73] Ebrahim AF, Ahmed, SMW, Elmasry SE, Mohammed OA. Implementation of a PV emulator using programmable DC power supply. In: SoutheastCon 2015; 2015, p. 1–7.

[74] Ollila J. A medium power PV-array simulator with a robust control strategy. In: Proceedings of the 4th IEEE Conference on Control applications; 1995. p. 40–5.

[75] Preethishri TPV, Kumar KS, Sivakumar P. Embedded emulator of photovoltaic array and wind driven induction generator by using digital signal controller (tms320f28335). In: Proceedings of the 2010 India international conference on power electronics (IICPE); 2011. p. 1.

[76] Wandhare RG, Agarwal V. A low cost, light weight and accurate photovoltaic emulator. In: Proceedings of the 2011 37th IEEE photovoltaic specialists conference (PVSC); 2011. p. 001887–92.

[77] Ding K, Bian X, Liu H, Peng T. A MATLAB-simulink-based PV module model and its application under conditions of nonuniform irradiance. Energy Convers IEEE Trans 2012;27:864–72.

[78] Leban K, Ritchie E. Selecting the accurate solar panel simulation model. In: Nordic workshop on power and industrial electronics (NORPIE/2008), June 9-11, 2008. Espoo, Finland; 2008.

[79] Walker G. Evaluating MPPT converter topologies using a MATLAB PV model. J Electr Electron Eng, Aust 2001;21:49–56.

[80] Yusof Y, Sayuti SH, Abdul Latif M, Wanik MZC. Modeling and simulation of maximum power point tracker for photovoltaic system. In: proceedings power and energy conference, national, 2004. PECon 2004; 2004 . p. 88–93.

[81] Patel BD, Rana A. A pole-placement approach for buck converter based PV array Emulator. In: Proceedings of the 2016 IEEE 1st international conference on power electronics, intelligent control and energy systems (ICPEICES); 2016. p. 1–5.

[82] Binduhewa PJ, Barnes M. Photovoltaic emulator. In: Proceedings of the 8th IEEE international conference on industrial and information systems (ICIIS); 2013. p. 519–24.

[83] Kamarzaman NA, Tan CW. A comprehensive review of maximum power point tracking algorithms for photovoltaic systems. Renew Sustain Energy Rev 2014;37:585–98, [9//].

[84] Khouzam K, Hoffman K. Real-time simulation of photovoltaic modules. Sol Energy 1996;56:521–6.

[85] Chin VJ, Salam Z, Ishaque K. Cell modelling and model parameters estimation techniques for photovoltaic simulator application: a review. Appl Energy 2015;154:500–19, [9/15/].

[86] Seo YT, Park JY, Choi SJ. A rapid I-V curve generation for PV model-based solar array simulators. In: Proceedings of ECCE 2016 - IEEE energy conversion congress and exposition; 2016.

[87] Yuncong J, Qahouq JAA, Batarseh I. Improved solar PV cell Matlab simulation model and comparison. In: Proceedings of 2010 IEEE international symposium on circuits and systems (ISCAS); 2010. p. 2770–3.

[88] Bellia H, Youcef R, Fatima M. A detailed modeling of photovoltaic module using MATLAB. NRIAG J Astron Geophys 2014;3:53–61, [6//].

[89] Djamila Rekioua EM. Optimization of photovoltaic power systems modelization, simulation and control. Verlag London: Springer; 2012.

[90] Can H, Ickilli D, Parlak KS, Ieee. A new numerical solution approach for the real-time modeling of photovoltaic panels. In: 2012 Asia-Pacific power and energy engineering conference. New York; 2012.

[91] Cordeiro A, Foito D, Fern V, o P. A PV panel simulator based on a two quadrant DC/DC power converter with a sliding mode controller. In: 2015 international conference on renewable energy research and applications (ICRERA); 2015. p. 928–32.

[92] Rachid A, Kerrour F, Chenni R, Djeghloud H. PV emulator based buck converter using dSPACE controller. In: Proceedings of the 16th international conference on environment and electrical engineering (EEEIC), 2016 IEEE; 2016. p. 1–6.

[93] Wei P, Tan B, Zhang H, Zhao Y. Research on maximum power point tracker based on solar cells simulator. In: Proceedings of the 2nd international conference on advanced computer control (ICACC); 2010 p. 319–3.

[94] Di Piazza MC, Vitale G. Photovoltaic field emulation including dynamic and partial shadow conditions. Appl Energy 2010;87:814–23, [3//].

[95] Chang C-H, Chang E-C, Cheng H-L. A high-efficiency solar array simulator implemented by an LLC resonant DC–DC converter. IEEE Trans Power Electron 2013;28:3039–46.

[96] Chan DSH, Phang JCH. Analytical methods for the extraction of solar-cell single- and double-diode model parameters from I-V characteristics. Electron Devices IEEE Trans 1987;34:286–93.

[97] Garai SK. A photovoltaic cell emulator. Kolkata, West Bengal, India: Master of Technology in Instrumentation & Electronics Engineering Department of Instrumentation and Electronics Engineering, Jadavpur University; 2013.

[98] Dolan DSL, Durago J, Taufik. Development of a photovoltaic panel emulator using Labview. In: Proceedings of the 2011 37th IEEE photovoltaic specialists conference (PVSC); 2011. p. 001795–800.

[99] Zhao J, Kimball JW. A digitally implemented photovoltaic simulator with a double current mode controller. In: Proceedings of the twenty-seventh annual ieee applied power electronics conference and exposition (APEC); 2012. p. 53–8.

[100] Koran AM. Photovoltaic source simulators for solar power conditioning systems: design optimization, modeling, and control. Blacksburg, Virginia: Doctor of Philosophy, Faculty of the Virginia Polytechnic Institute and State University, Virginia Polytechnic Institute and State University; 2013.

[101] Iqbal MT, Tariq M, Khan MSU. Fuzzy logic control of buck converter for photo voltaic emulator. In: Proceedings of the 4th international conference on the development in the in renewable energy technology (ICDRET); 2016. p. 1–6.

[102] Bhise K, Pragallapati N, Thale S, Agarwal V. Labview based emulation of photovoltaic array to study maximum power point tracking algorithms. In: Proceedings of the 2012 38th IEEE photovoltaic specialists conference (PVSC); 2012. p. 002961–6.

[103] Chavarría J, Biel D, Guinjoan F, Poveda A, Masana F, Alarcón E. FPGA-based design of a step-up photovoltaic array emulator for the test of PV grid-connected inverters. In: Proceedings of the 2014 IEEE 23rd international symposium on industrial electronics (ISIE); 2014. p. 485–90.

[104] Masashi S, Naoki Y, Muneaki I. Development of Photovoltaic cell emulator using the small scale wind turbine. In: Proceedings of the 15th international conference on electrical machines and systems (ICEMS); 2012. p. 1–4.

[105] Algaddafi A, Brown N, Gammon R, Altuwayjiri SA. Effect of PV array emulator on power quality of PV inverter compared to a real PV array. In: Proceedings of the 3rd international renewable and sustainable energy conference (IRSEC); 2015, p. 1–6.

[106] Nanakos AC, Tatakis EC. Static and dynamic response of a photovoltaic characteristics simulator. In: Proceedings of the 13th power electronics and motion control conference, EPE-PEMC; 2008. p. 1827–33.

[107] Ayop R, Tan CW. An adaptive controller for photovoltaic emulator using artificial neural network. Indones J Electr Eng Comput Sci 2017;5:556–63.

[108] Duru ÖÖY, Zengin S, Boztepe M. Design and implementation of programmable PV simulator. In: Proceedings of the 2016 international symposium on fundamentals of electrical engineering (ISFEE); 2016. p. 1–5.

[109] Nagayoshi H. Characterization of the module/array simulator using IV magnifier circuit of a pn photo-sensor. In: Proceedings of the 3rd world conference on photovoltaic energy conversion; 2003. p. 2023–6.

[110] Nagayoshi H, Orio S, Kono Y, Nakajima H. Novel PV array/module I-V curve simulator circuit. In: Conference record of the twenty-ninth IEEE photovoltaic specialists conference; 2002. p. 1535–8.

[111] Mukerjee AK, Dasgupta N. DC power supply used as photovoltaic simulator for testing MPPT algorithms. Renew Energy 2007;32:587–92, [4//].

[112] Lopes LA, Lienhardt A-M. A simplified nonlinear power source for simulating PV panels. In: Proceedings of the 2003 IEEE 34th annual power electronics specialist conference. PESC'03; 2003. p 1729–34.

[113] Hart DW. Power electronics. 1221 Avenue of the Americas, New York, NY 10020: Valparaiso University, Indiana: Tata McGraw-Hill Education; 2011.

[114] Soetedjo A, Nakhoda YI, Lomi A, Hendroyono GE. Development of PV simulator by integrating software and hardware for laboratory testing. In: 2015 international conference on automation, cognitive science, optics, micro electro-mechanical system, and information technology (ICACOMIT); 2015. p. 96–100.

[115] Kadri R, Andrei H, Gaubert J-P, Ivanovici T, Champenois G, Andrei P. Modeling of the photovoltaic cell circuit parameters for optimum connection model and real-time emulator with partial shadow conditions. Energy 2012;42:57–67, [6//].

[116] Sanyo . L. Sanyo Electric Co. , editor. Sanyo HIT photovoltaic module. Stahlgruberring 4, 81829 Munich, Germany: SANYO Component Europe GmbH, Solar Division; 2009.

[117] Wang K, Li Y, Rao J, Sun M. Design and implementation of a solar array simulator. In: International conference on electrical machines and systems, 2008 ICEMS 2008; 2008. p. 2633–6.

[118] Kulkarni SS, Thean CY, Kong AW. A novel PC based solar electric panel simulator. In: . In: Proceedings of the fifth international conference on power electronics and drive systems, 2003. PEDS 2003. Vol. 2; 2003. p. 848–52.

[119] Thale S, Wandhare R, Agarwal V. A novel low cost portable integrated solar PV, fuel cell and battery emulator with fast tracking algorithm. In: Proceedings of photovoltaic specialist conference (PVSC), 2014 IEEE 40th; 2014. p. 3138–43.

[120] Lattanzi E, Dromedari M, Freschi V, Bogliolo A. Tuning the complexity of photovoltaic array models to meet real-time constraints of embedded energy emulators. Energies 2017;10.

[121] Floyd TL. Electronic devices, 9th edition. Prentice Hall, 1 Lake Street, Upper Saddle River, New Jersey: Pearson; 2012.

[122] Chavarría J, Biel D, Guinjoan F, Poveda A, Masana F, Alarcon E. Low cost photovoltaic array emulator design for the test of PV grid-connected inverters. In: Proceedings of 2014 11th international multi-conference on systems, signals & devices (SSD); 2014. p. 1–6.

[123] Pressman A. Switching power supply design, 3. New York: McGraw-Hill, Inc; 1997.

[124] Ilic M, Maksimovic D. Interleaved zero-current-transition buck converter. Ind Appl IEEE Trans 2007;43:1619–27.

[125] Garcia J, Calleja AJ, Gacio Vaquero D, Campa L. Interleaved buck converter for fast PWM dimming of high-brightness LEDs. Power Electron IEEE Trans 2011;26:2627–36.

[126] Bendali M, Larouci C, Azib T, Marchand C, Coquery G. Design methodology with optimization of an interleaved buck converter for automotive application. In: EUROCON, 2013 IEEE; 2013. p. 1066–72.

[127] Qiu Y, Xu M, Yao K, Sun J, Lee FC. Multifrequency small-signal model for buck and multiphase buck converters. IEEE Trans Power Electron 2006;21:1185–92.

[128] García O, Zumel P, De Castro A, Cobos JA. Automotive DC-DC bidirectional converter made with many interleaved buck stages. Power Electron IEEE Trans 2006;21:578–86.

[129] Jang Y, Jovanovic MM, Panov Y. Multiphase buck converters with extended duty cycle. In: Proceedings IEEE applied power electronics conference(APEC'06); 2006. p. 38–44.

[130] Esteki M, Poorali B, Adib E, Farzanehfard H. Interleaved buck converter With continuous input current, extremely low output current Ripple, low switching losses, and improved step-down conversion ratio. Ind Electron IEEE Trans 2015;62:4769–76.

[131] Lee I-O, Cho S-Y, Moon G-W. Interleaved buck converter having low switching losses and improved step-down conversion ratio. Power Electron IEEE Trans 2012;27:3664–75.

[132] Cacciato M, Consoli A, Scarcella G, Testa A. A multhi-phase DC/DC converter for automotive dual-voltage power systems. IEEE Ind Appl Mag 2004;40:2–9.

[133] Esteki M, Poorali B, Adib E, Farzanehfard H. High step-down interleaved buck converter with low voltage stress. Power Electron IET 2015;8:2352–60.

[134] Heredero-Peris D, Capo-Lliteras M, Miguel-Espinar C, Lledo-Ponsati T, Montesinos-Miracle D. Development and implementation of a dynamic PV emulator with HMI interface for high power inverters. In: Proceedings of the 16th European conference on power electronics and applications (EPE'14-ECCE Europe); 2014. p. 1–10.

[135] Kazimierczuk MK. Pulse-width modulated DC-DC power converters. Dayton, Ohio, USA: Wiley. Wright State University; 2008.

[136] Erickson RW, Maksimovic D. Fundamentals of power electronics, 2 ed. New York, Boston, Dordrecht, London, Moscow: Kluwer Academic Publishers; 2004.

[137] Bacha S, Munteanu I, Bratcu AI. Power electronic converters modeling and control: with case studies. London: Springer-Verlag; 2014.

[138] Chetty P. Current injected equivalent circuit approach to modeling of switching DC-DC converters in discontinuous inductor conduction mode. IEEE Trans Ind Electron 1982;3:230–4.

[139] Vorperian V. Simplified analysis of PWM converters using model of PWM switch. II. Discontinuous conduction mode. Aerosp Electron Syst IEEE Trans 1990;26:497–505.

[140] Wester GW, Middlebrook RD. Low-frequency characterization of switched dc-dc converters. Aerosp Electron Syst IEEE Trans 1973;AES-9:376–85.

[141] Suman G, Kumar BVSP, Kumar MS, Babu BC, Subhashini KR. Modeling, analysis and design of synchronous buck converter using state space averaging technique for PV energy system. In: Proceedings of the 2012 international symposium on electronic system design (ISED); 2012. p. 281–5.

[142] Jingquan C, Erickson R, Maksimovic D. Averaged switch modeling of boundary conduction mode DC-to-DC converters. In: Proceedings of the 27th Annual Conference of the IEEE Industrial electronics society, 2001. IECON '01. Vol. 2; 2001. p. 844–49.

[143] Cuk S, Middlebrook RD. A general unified approach to modelling switching DC-tO-DC converters in discontinuous conduction mode. In: 1977 IEEE power electronics specialists conference; 1977, p. 36–57.

[144] Kasat S. Analysis, design and modeling of DC-DC converter using simulink. Stillwater, Oklahoma: Master of Science, Institute of Engineering and Technology Oklahoma State University; 2004.

[145] Abdullah MA, Tan CW, Yatim AH, Al-Mothafar M, Radaideh SM. Input current control of boost converters using current-mode controller integrated with linear quadratic regulator. Int J Renew Energy Res (IJRER) 2012;2:262–8.

[146] Nise NS. Control systems engineering, 6th edition. Chichester, United Kingdom: California State Polytechnic University, Pomona WJohn Wiley & Sons, Inc.; 2011.